© 2014. Published by The Company of Biologists Ltd | Journal of Cell Science (2014) 127, 2269–2281 doi:10.1242/jcs.140905

RESEARCH ARTICLE

FHL1 mutants that cause clinically distinct human myopathies form protein aggregates and impair myoblast differentiation

Brendan R. Wilding[1], Meagan J. McGrath[1], Gisèle Bonne[2,3,4] and Christina A. Mitchell[1,*]

ABSTRACT

FHL1 mutations cause several clinically heterogeneous myopathies, including reducing body myopathy (RBM), scapuloperoneal myopathy (SPM) and X-linked myopathy with postural muscle atrophy (XMPMA). The molecular mechanisms underlying the pathogenesis of FHL1 myopathies are unknown. Protein aggregates, designated 'reducing bodies', that contain mutant FHL1 are detected in RBM muscle but not in several other *FHL1* myopathies. Here, RBM, SPM and XMPMA FHL1 mutants were expressed in C2C12 cells and showed equivalent protein expression to wild-type FHL1. These mutants formed aggregates that were positive for the reducing body stain Menadione-NBT, analogous to RBM muscle aggregates. However, hypertrophic cardiomyopathy (HCM) and Emery-Dreifuss muscular dystrophy (EDMD) FHL1 mutants generally exhibited reduced expression. Wild-type FHL1 promotes myoblast differentiation; however, RBM, SPM and XMPMA mutations impaired differentiation, consistent with a loss of normal FHL1 function. Furthermore, SPM and XMPMA FHL1 mutants retarded myotube formation relative to vector control, consistent with a dominant-negative or toxic function. Mutant FHL1 myotube formation was partially rescued by expression of a constitutively active FHL1-binding partner, NFATc1. This is the first study to show that *FHL1* mutations identified in several clinically distinct myopathies lead to similar protein aggregation and impair myotube formation, suggesting a common pathogenic mechanism despite heterogeneous clinical features.

KEY WORDS: FHL1, Myopathy, RBM, SPM, XMPMA

INTRODUCTION

The four and a half LIM domain protein 1 (FHL1) is highly expressed in skeletal and cardiac muscle (Lee et al., 1998; Brown et al., 1999; Greene et al., 1999; Morgan and Madgwick, 1999), influencing cellular architecture (McGrath et al., 2003; McGrath et al., 2006), myoblast differentiation (Lee et al., 2012), mechanotransduction (Sheikh et al., 2008) and skeletal-muscle fibre size (Cowling et al., 2008). FHL1 mediates protein–protein interactions through its LIM domains; cysteine-rich double zinc fingers containing the consensus sequence [CX2CX16-23HX2C] X2 [CX2CX16-21CX2(C/H/D)] that facilitate binding to proteins but not DNA (Schmeichel and Beckerle, 1997). The highly conserved cysteine and histidine residues mediate Zn^{2+} binding, which stabilises the folding and structure of the LIM domain. FHL1 binds to signalling and cytoskeletal proteins, as well as transcription factors, acting as a transcriptional regulator of nuclear factor of activated T cells (NFATc1) to enhance the expression of genes that increase skeletal-muscle fibre size (Cowling et al., 2008).

FHL1 is mutated in six clinically distinct human myopathies, including reducing body myopathy (RBM) (Schessl et al., 2008; Schessl et al., 2009; Shalaby et al., 2009; Schessl et al., 2010; Selcen et al., 2011; Schreckenbach et al., 2013), X-linked dominant scapuloperoneal myopathy (SPM) (Quinzii et al., 2008; Chen et al., 2010), X-linked myopathy with postural muscle atrophy (XMPMA) (Windpassinger et al., 2008), rigid-spine syndrome (RSS) (Shalaby et al., 2008), hypertrophic cardiomyopathy (HCM) (Friedrich et al., 2012) and Emery-Dreifuss muscular dystrophy (EDMD) (Gueneau et al., 2009; Knoblauch et al., 2010). In RBM, both missense and deletion mutations affecting cysteine and histidine residues in FHL1 LIM domain-2 have been reported (see Fig. 1). RBM generally exhibits dominant inheritance with progressive muscle loss, rigid spine, scapular winging and contractures, and, in some cases, severe infantile and childhood onset with rapid progression and cardiac/respiratory failure (reviewed in Cowling et al., 2011). RBM is distinguished by the presence of intracellular protein aggregates called 'reducing bodies' in affected muscle, which stain positively with Menadione-NBT (M-NBT). Reducing bodies contain mutated FHL1 protein, cytoskeletal and intermediate filament proteins and components of the unfolded protein response (UPR) (Liewluck et al., 2007). Reducing bodies morphologically resemble aggresomes – structures proposed to facilitate the sequestration and degradation of toxic misfolded protein (reviewed in Kopito, 2000). SPM, XMPMA, RSS, HCM and EDMD are associated with variable FHL1 protein expression in affected muscle, from normal levels to reduced or absent (see supplementary material Table S1). Although SPM, XMPMA, RSS, HCM and EDMD share some overlapping clinical features and muscle pathology with RBM, the involvement of protein aggregation in these disorders remains unclear. SPM muscle exhibits desmin-positive cytoplasmic inclusions that occasionally stain positively for FHL1; however, reducing bodies have not been reported (Quinzii et al., 2008; Chen et al., 2010). SPM FHL1 mutations do not directly affect zinc-binding residues, rather an adjacent conserved tryptophan residue in LIM domain-2 is mutated to serine or cysteine (W122S/C). Similarly, XMPMA mutations do not affect conserved LIM domain-2 zinc-binding residues, rather an isoleucine is inserted within the conserved-length dipeptide linker between adjacent zinc fingers in LIM 2 (127-I-128) or missense mutations affect zinc-coordinating residues in LIM domain-4 (C224W, H246Y) (Windpassinger et al., 2008; Schoser et al., 2009). XMPMA shows an almost

[1]Department of Biochemistry & Molecular Biology, Faculty of Medicine, Nursing & Health Sciences, Monash University, Clayton, VIC 3800, Australia. [2]Inserm, U974, Paris, F-75013, France. [3]Université Pierre et Marie Curie-Paris 6, UM 76, CNRS, UMR7215, Institut de Myologie, IFR14, Paris, F-75013, France. [4]AP-HP, Groupe Hospitalier Pitié-Salpêtrière, U.F. Cardiogénétique et Myogénétique Moléculaire, Service de Biochimie Métabolique, Paris, F-75013, France.

*Author for correspondence (christina.mitchell@monash.edu)

Received 15 August 2013; Accepted 14 February 2014

Journal of Cell Science (2014) 127, 2269–2281 doi:10.1242/jcs.140905

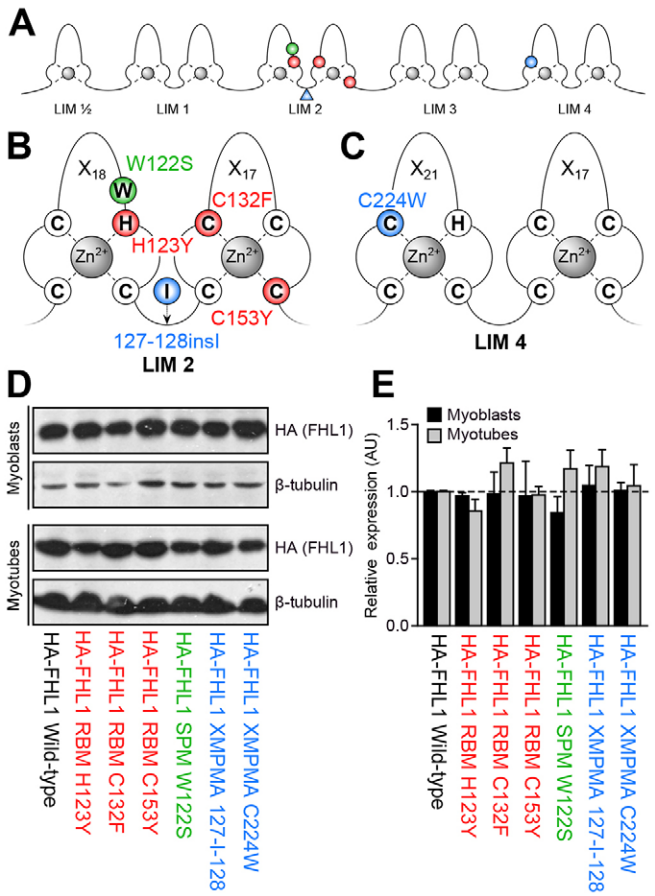

Fig. 1. Mutant FHL1 protein expression is similar to wild-type FHL1 expression *in vitro*. (A) FHL1 point and insertion mutations identified in RBM (red), SPM (green) and XMPMA (blue) affect LIM domain-2 (B) and LIM domain-4 (C). (D) C2C12 myoblasts were transiently transfected with HA-tagged wild-type FHL1, RBM H123Y, RBM C132F, RBM C153Y, SPM W122S, XMPMA 127-I-128, or XMPMA C224W, and whole-cell lysates were immunoblotted with anti-HA or anti-β-tubulin antibodies after 24 hours of expression (myoblasts) and after 72 hours of differentiation (myotubes). (E) HA–FHL1 expression was analysed by densitometry, quantified relative to the β-tubulin loading control and represented relative to that of wild-type HA–FHL1 (dashed black line). Data represent the mean±s.e.m.; $n=3$.

complete absence of mutant FHL1 protein by western blot analysis of affected muscles. XMPMA muscle exhibits desmin-positive bodies; however, affected muscle was initially reported not to contain reducing bodies. Interestingly, a three-amino-acid deletion in LIM domain-2 that is associated with RSS exhibits reduced FHL1 protein expression and FHL1 protein accumulations are observed (Shalaby et al., 2008). This myopathy probably represents a milder clinical form of RBM. EDMD and HCM FHL1 mutations include missense, frame-shift and truncation mutations that result in reduced expression or absence of FHL1 protein in affected muscle, and accumulation of mutant FHL1 protein or reducing bodies have not been reported (Gueneau et al., 2009; Knoblauch et al., 2010; Friedrich et al., 2012).

The molecular basis of how *FHL1* mutations cause these clinically distinct human myopathies remains unclear, and there are currently no therapies. Whether all mutant forms of FHL1 aggregate and what function these aggregates impart might be significant in terms of disease pathogenesis. Here, using *in vitro* ectopic expression of FHL1 mutants in C2C12 cells, we demonstrate that RBM, SPM and XMPMA FHL1 mutants all form protein aggregates analogous to the M-NBT-positive reducing bodies observed in RBM muscle; however, EDMD and HCM FHL1-mutant protein expression is significantly reduced. Furthermore, RBM, SPM and XMPMA mutants impaired myoblast fusion and differentiation relative to wild-type FHL1, which leads to myotube hypertrophy. Wild-type FHL1 promotes myoblast fusion and differentiation by regulating NFATc1 transcriptional activity, and we have previously reported that NFATc1 is trapped within aggregates of mutant FHL1 in RBM (Cowling et al., 2008; Schessl et al., 2008). Notably, we show here that mutant-FHL1-induced myoblast differentiation defects are rescued by expression of constitutively active NFATc1, suggesting that *FHL1* myopathies are caused by dominant-negative mutant FHL1 function or by the gain of a new toxic function.

RESULTS

SPM and XMPMA FHL1 mutants accumulate *in vitro* and form reducing body aggregates

Many clinical studies have reported that FHL1 protein shows variable levels of expression in affected muscle in clinically distinct FHL1-mutant myopathies (see supplementary material Table S1). Here, we investigated the relative expression of FHL1 mutants and their ability to form reducing body aggregates *in vitro* in C2C12 myoblasts. Representative examples of clinically distinct FHL1-myopathy mutants were generated, including RBM (H123Y, C132F and C153Y), SPM (W122S) and XMPMA (127-I-128 and C224W) (Fig. 1A–C). C2C12 skeletal myoblasts were transiently transfected with the HA–FHL1 mutants or with wild-type HA–FHL1, and myoblasts were differentiated into myotubes for 72 hours. HA–FHL1 expression was determined by western blot analysis using antibodies against the HA tag. Surprisingly, the expression of SPM and both XMPMA FHL1 mutants was equivalent to wild-type HA–FHL1 expression in both myoblasts and myotubes at similar time-points following transfection (Fig. 1D,E). RBM FHL1 mutants also expressed at equivalent levels. No significant differences ($P<0.05$) between wild-type HA–FHL1 and mutant HA–FHL1 expression were identified.

We previously reported that the RBM-associated H123Y and C132F FHL1 mutants in C2C12 cells *in vitro* form intracellular accumulations, which are positive for M-NBT staining, analogous to aggregates containing endogenous mutant FHL1 in RBM-affected muscle (Schessl et al., 2008). However, it is unclear whether FHL1 mutant aggregation is progressive during myoblast differentiation into myotubes (given the rapid progressiveness of RBM myopathy) and whether other FHL1 mutants also aggregate; especially non-RBM clinically classified disease-associated mutants. We therefore assessed the aggregation propensity of RBM, SPM and XMPMA FHL1 mutants in differentiating C2C12 cells, by examining the subcellular localisation of mutant FHL1 using immunofluorescence microscopy. The RBM-associated H123Y and C132F FHL1 mutants were diffusely cytoplasmic in myoblasts (at 0 hours differentiation, 24 hours FHL1 expression); however, by 72 hours of differentiation, accumulations of mutant FHL1 were observed in ~30% of RBM-mutant-expressing myotubes (Fig. 2A,B). The previously uncharacterised RBM-associated C153Y FHL1 mutant also formed accumulations in myotubes, comparable to other RBM FHL1 mutants. All RBM FHL1 mutants progressively formed accumulations that were

Journal of Cell Science (2014) 127, 2269–2281 doi:10.1242/jcs.140905

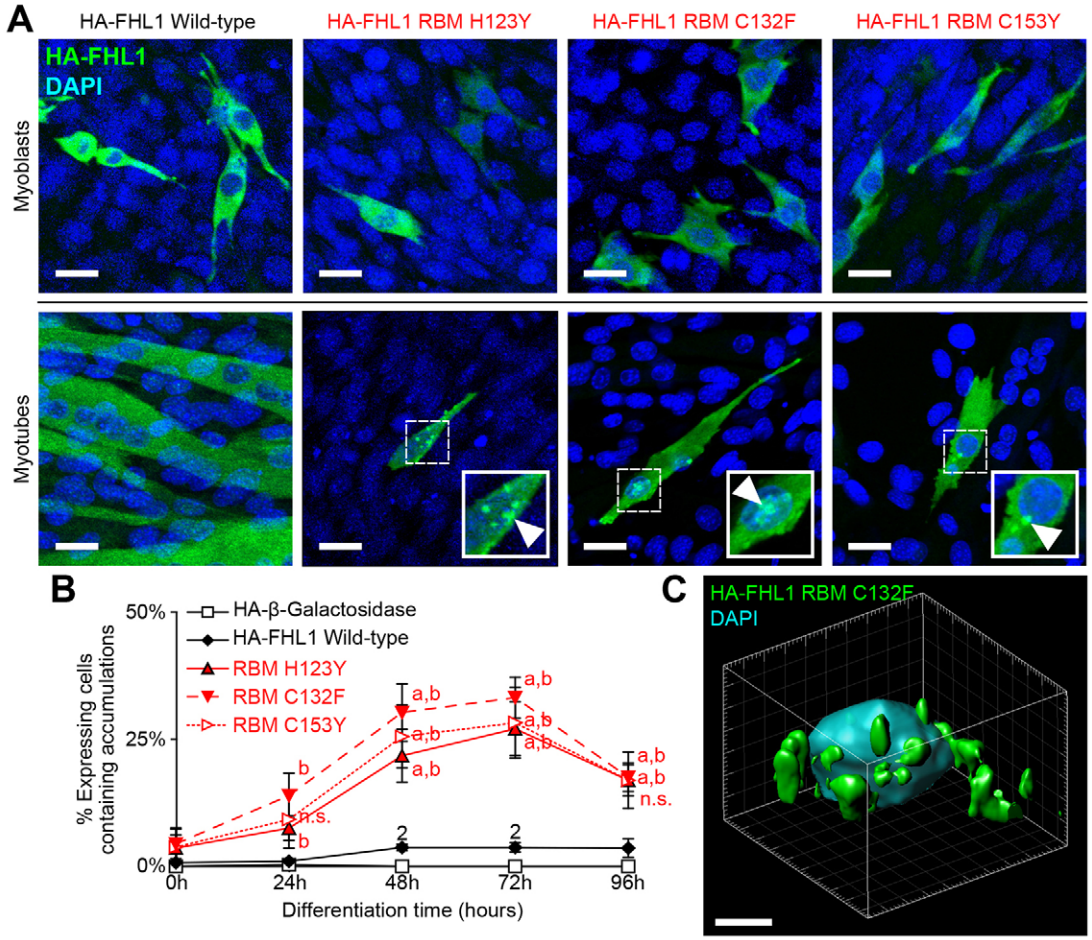

Fig. 2. RBM FHL1 mutants form perinuclear accumulations in myotubes but not myoblasts. (A) C2C12 myoblasts transiently transfected with RBM mutant HA–FHL1 (H123Y, C132F or C153Y) or wild-type HA–FHL1 were differentiated for 72 hours, co-stained with anti-HA (green) and DAPI (nuclei, blue), and imaged by fluorescence confocal microscopy. Inset, 2× magnification of dashed box; arrowheads, mutant HA–FHL1 accumulation. (B) The percentage of HA–FHL1-expressing cells that contain HA–FHL1 accumulations was scored. Cells were visually scored as positive if at least one focus of fluorescence intensity greater than cytoplasmic fluorescence staining was observed. Data represent the mean±s.e.m.; ≥100 cells per independent experiment; $n \geq 3$; $^{a}P<0.05$ compared with wild-type HA–FHL1; $^{b}P<0.05$ compared with β-galactosidase control; n.s., not significant. (C) Surface rendering of mutant HA–FHL1 (green) and adjacent myonuclei (DAPI, blue) analysed by fluorescence intensity threshold. Scale bars: 25 μm (A), 5 μm (C).

predominantly perinuclear (Fig. 2C); however, peripheral cytoplasmic accumulations were also present. Importantly, wild-type HA–FHL1 rarely accumulated in myotubes (<4% of expressing cells), and no accumulations were present in myotubes expressing an HA-tagged β-galactosidase (β-gal) vector control.

Interestingly, SPM (W122S) and XMPMA (127-I-128, C224W) FHL1 mutants formed accumulations in myotubes (Fig. 3A) that were rarely observed in myoblasts (not shown), but the percentage of cells containing these accumulations increased with expression time and myoblast differentiation (Fig. 3B), equivalent to RBM FHL1 mutants. Although the accumulations were predominantly perinuclear (Fig. 3C), peripheral accumulations were also observed. We therefore analysed specific markers of reducing body aggregates within the accumulations of SPM and XMPMA mutant FHL1 in myotubes. Reducing bodies are characterised by strong M-NBT staining that colocalises with UPR-mediator proteins and other aggresomal proteins. Interestingly, SPM and XMPMA FHL1 mutants formed perinuclear accumulations (Fig. 4a–d) that stained positively with M-NBT (Fig. 4e–h), indicating that SPM and XMPMA FHL1 mutants form ‘reducing-body-like’ aggregates. The UPR is induced by misfolded intracellular protein, as a mechanism to reduce the accumulation of misfolded protein by increasing the levels of the protein-folding machinery, promoting protein-degradative machinery and inhibiting global translation (reviewed in Wang and Kaufman, 2012). The protein chaperone and stress sensor GRP78 (also known as HSPA5 or BiP) binds to misfolded proteins and initiates UPR signalling. Protein degradation is mediated by proteasomal degradation of ubiquitin-tagged misfolded protein. The reducing bodies that are associated with RBM-afflicted muscle colocalise with GRP78 and ubiquitin (Liewluck et al., 2007). Notably, the UPR marker GRP78 and ubiquitin exhibited enriched colocalisation with HA–FHL1 RBM, SPM and XMPMA mutant aggregates (Fig. 4i–l). Although mutant FHL1 colocalised with ubiquitin, mutant FHL1 protein expression was similar to wild-type HA–FHL1 within this time frame (Fig. 1D). In control studies, no difference in the expression levels of GRP78 were detected by western blotting under conditions of mutant FHL1 expression (not shown).

Journal of Cell Science (2014) 127, 2269–2281 doi:10.1242/jcs.140905

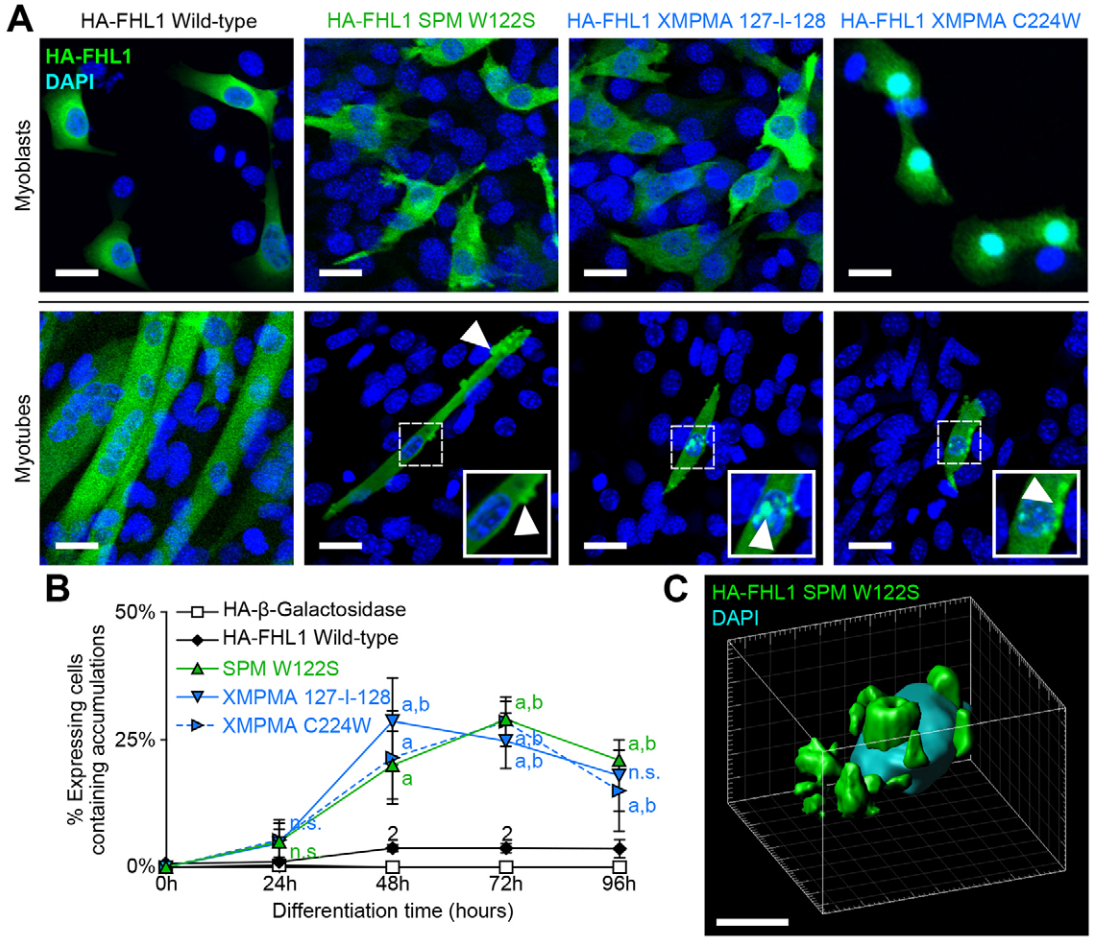

Fig. 3. SPM and XMPMA mutant FHL1 accumulates in myotubes. (A) C2C12 myoblasts transiently transfected with HA–FHL1 SPM W122S, XMPMA 127-I-128, XMPMA C224W or wild-type HA–FHL1 were differentiated for 72 hours, co-stained with anti-HA (green) and DAPI (nuclei, blue) and imaged by fluorescence confocal microscopy. Inset, 2× magnification of dashed box; arrowheads, mutant HA–FHL1 accumulation. (B) The percentage of HA–FHL1-expressing cells that contain HA–FHL1 accumulations was scored. Cells were visually scored as positive if at least one focus of fluorescence intensity greater than cytoplasmic fluorescence staining was observed. Data represent the mean±s.e.m.; ≥100 cells per independent experiment; $n \geq 3$; $^{a}P<0.05$ compared with wild-type HA–FHL1; $^{b}P<0.05$ compared with β-galactosidase control; n.s., not significant. (C) Surface rendering of mutant HA–FHL1 (green) and adjacent myonuclei (DAPI, blue) analysed by fluorescence intensity threshold. Scale bars: 25 μm (A), 5 μm (C).

FHL1 three-amino-acid deletions identified in RSS and RBM accumulate *in vitro*

FHL1 mutations might affect conserved zinc-ion-binding residues that are crucial for the integrity of the LIM domain or the mutations might occur outside the LIM domain. This is proposed to dictate both disease severity and/or the expression level of mutant FHL1 protein (reviewed in Cowling et al., 2011). SPM and XMPMA FHL1 mutations show reduced FHL1 expression, do not affect LIM 2 zinc-binding residues and are milder compared with RBM. By contrast, LIM domain-2 missense mutations in RBM generally exhibit FHL1 protein expression that is similar to wild-type levels but show a clinically more-severe myopathy. Clinically less-severe three-amino-acid deletions affecting the zinc-binding cysteine residues in FHL1 LIM domain-2 have been identified in RBM and RSS. The three-amino-acid-deletion mutant FHL1 RBM 102–104delKGC (102–104Δ) is associated with increased expression of mutant FHL1 protein in afflicted muscle and exhibits classical formation of reducing bodies (Shalaby et al., 2009); however, another three-amino-acid-deletion mutant, FHL1 RSS 151–153delVTC (151–153Δ), exhibits reduced expression of mutant FHL1 protein yet the formation of reducing bodies occurs in affected muscle (Shalaby et al., 2008). We investigated whether the FHL1 three-amino-acid-deletion mutants RBM 102–104Δ and RSS 151–153Δ (Fig. 5A) showed altered ectopic FHL1 protein expression in C2C12 cells and/or were associated with aggregation of mutant FHL1 protein. FHL1 RBM 102–104Δ expression was similar to wild-type HA–FHL1 protein expression in myoblasts and myotubes, as was protein expression of FHL1 RSS 151–153Δ, although the latter was occasionally reduced in myotubes (although this was not statistically significant) (Fig. 5B). Notably, the expression of either three-amino-acid-deletion mutant was associated with mutant FHL1 accumulation at comparable levels and with similar subcellular distribution to that observed for RBM, SPM and XMPMA FHL1 mutants (Fig. 5C,D). The three-amino-acid-deletion mutants also co-stained with ubiquitin (not shown).

FHL1 missense, frameshift and loss-of-stop-codon mutations identified in EDMD exhibit variable protein expression of mutant FHL1 and accumulate *in vitro*

We have previously reported that frameshift and truncation FHL1 mutations identified in hypertrophic cardiomyopathy (HCM) lead to the degradation of mutant FHL1 protein *in vitro*, resulting in

Journal of Cell Science (2014) 127, 2269–2281 doi:10.1242/jcs.140905

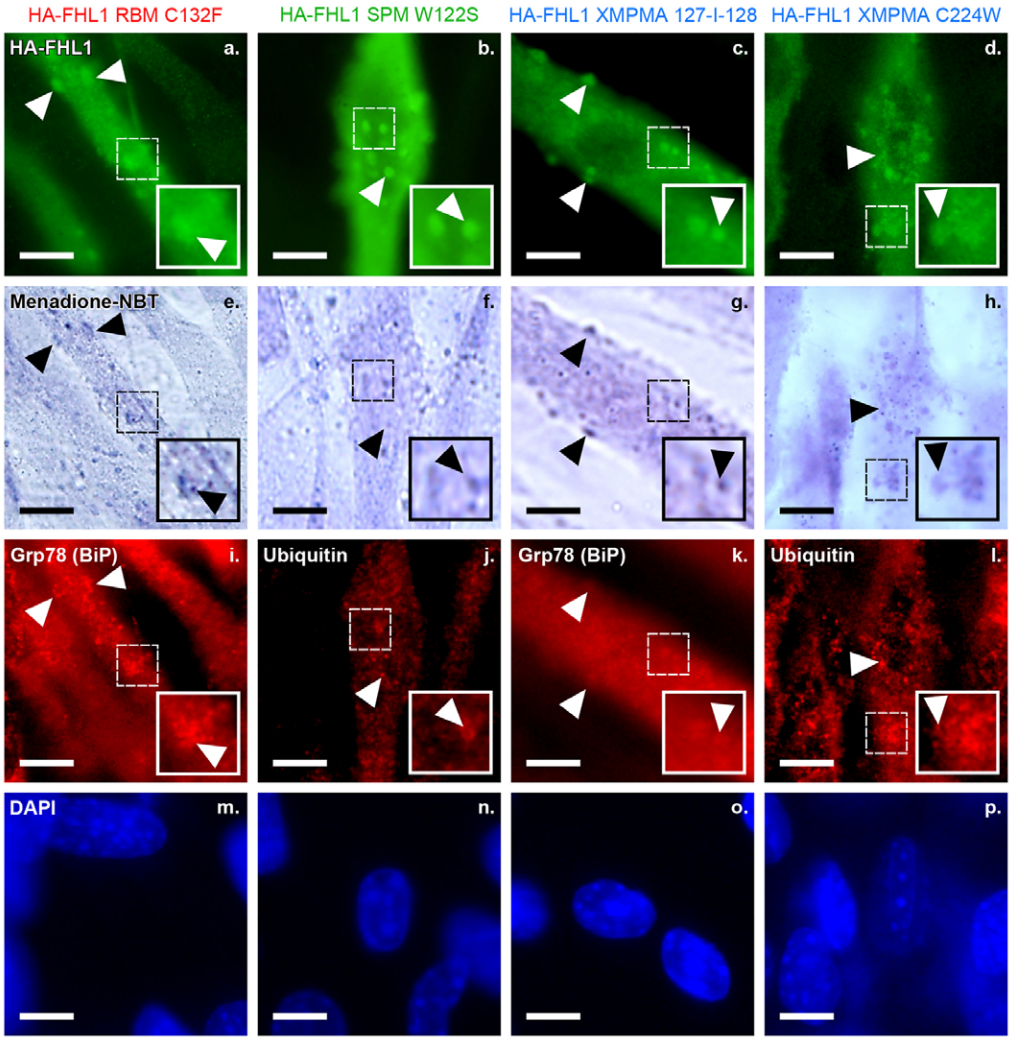

Fig. 4. SPM and XMPMA mutant FHL1 accumulations stain positively for reducing body markers. C2C12 myoblasts were transiently transfected with HA–FHL1 RBM C132F, SPM W122S, XMPMA 127-I-128 or C224W, and were differentiated for 72 hours. Myotubes were fixed, co-stained with anti-HA (a–d), Menadione-NBT in the absence of substrate (e–h), Grp78 (BiP) or ubiquitin (i–l) and DAPI (m–p), and imaged by wide-field fluorescence microscopy and brightfield microscopy. Arrowheads, accumulations of mutant FHL1 protein that co-stain with M-NBT and Grp78 or ubiquitin. Inset, 2× magnification of dashed box. Scale bars: 10 μm.

loss of FHL1 protein expression, which is partly rescued by proteasome inhibition (Friedrich et al., 2012). These mutants also aggregated in cardiomyocytes. A LIM domain-3 missense mutation identified in HCM with 'Emery-Dreifuss-like syndrome' exhibited reduced expression of mutant FHL1 in skeletal muscle (Knoblauch et al., 2010). Frameshift, loss-of-stop-codon and FHL1 LIM domain-4 point mutations are associated with reduced expression of mutant FHL1 protein in EDMD-affected skeletal muscle (Gueneau et al., 2009). As these mutations might represent a different class of mutation compared with RBM, SPM and XMPMA (notably, frameshift mutations) (Fig. 6A), we investigated whether FHL1 EDMD (111–229delinsG, K157VfsX36, C276Y, C273LfsX11, X281E) and HCM/EDMD (C209R) mutants showed altered FHL1 protein expression and/or were associated with the aggregation of mutant FHL1 protein *in vitro*. Notably, the frameshift and loss-of-stop-codon mutants C273LfsX11, K157VfsX36 and X281E exhibited almost absent protein expression (Fig. 6B,C), which could be partially restored by the proteasome inhibitor MG132 (supplementary material Fig. S1), similar to the HCM FHL1 mutation K45SfsX105 reported previously (Friedrich et al., 2012). The missense mutations C209R and C276Y showed reduced protein expression (0.59- and 0.81-fold, respectively, compared with wild-type HA–FHL1) but, surprisingly, the 111–229delinsG (111–229Δ) FHL1 mutant expressed at 3.35-fold relative to wild-type FHL1 overexpression. Notably, expression of all HCM/EDMD FHL1 mutants led to FHL1 accumulations in myotubes (Fig. 6D).

RBM, SPM and XMPMA FHL1 mutants are unable to enhance myotube formation

How *FHL1* mutations result in myopathies of varying severity and clinical presentation is currently unknown, and whether this represents a loss of function has not been explored. We previously reported that ectopic expression of wild-type FHL1 in C2C12 myoblasts increases myoblast fusion and myotube width, and transgenic FHL1 expression in murine skeletal muscle increases fibre size *in vivo* (Cowling et al., 2008). Ectopic expression of the RBM-associated FHL1 mutations H123Y and C132F in C2C12 cells impairs myoblast fusion and reduces myotube width relative to that of cells expressing wild-type FHL1 (Cowling et al., 2008). However, whether SPM, XMPMA and RSS FHL1 mutations also affect myotube formation is unclear, and might differ for clinically distinct FHL1 disease mutants. To address this question, representative FHL1 myopathy mutants from RBM, SPM, XMPMA and RSS were expressed in C2C12 myoblasts, and differentiation was induced for 72 hours. Myotube formation was assessed by staining myotubes with

Journal of Cell Science (2014) 127, 2269–2281 doi:10.1242/jcs.140905

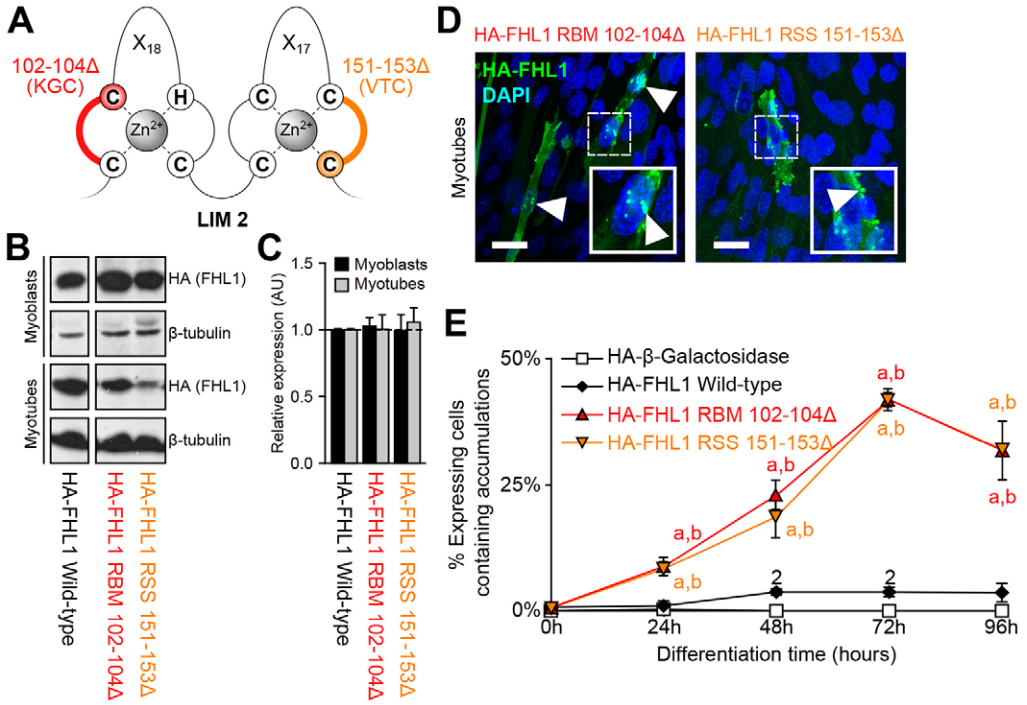

Fig. 5. FHL1 RBM and RSS deletion mutants form aggregates. (A) FHL1 three-amino-acid deletions identified in RBM (red) and RSS (orange) affect LIM domain-2 cysteine and adjacent residues. (B) C2C12 myoblasts were transiently transfected with HA-tagged wild-type FHL1, RBM 102–104Δ or RSS 151–153Δ, and whole-cell lysates were immunoblotted with anti-HA and anti-β-tubulin antibodies after 24 hours of expression (myoblasts) and after 72 hours of differentiation (myotubes). The wild-type FHL1 lane is the same as that shown in Fig. 1D, as wild-type and all FHL1 mutants in Fig. 1D and Fig. 5B were run on the same gel. (C) HA–FHL1 immunoblots were analysed by densitometry, quantified relative to the β-tubulin loading control and represented relative to wild-type HA–FHL1 (dashed black line). Data represent the mean±s.e.m.; $n=3$. (D) Myotubes differentiated for 72 hours were co-stained with anti-HA (green) and DAPI (nuclei, blue), and imaged by fluorescence confocal microscopy. Inset, 2× magnification of dashed box; arrowheads, mutant HA–FHL1 accumulation. Scale bars: 25 μm. (E) The percentage of HA–FHL1-expressing cells that contain HA–FHL1 accumulations were scored. Cells were scored positive if at least one focus of fluorescence intensity greater than cytoplasmic fluorescence staining was observed. Data represent the mean±s.e.m.; ≥100 cells per independent experiment; $n\geq3$; $^{a}P<0.05$ compared with wild-type HA–FHL1; $^{b}P<0.05$ compared with β-galactosidase control.

myosin heavy chain (MHC) and staining myonuclei with DAPI. Myotubes expressing wild-type HA–FHL1 appeared to be larger compared with those expressing HA–β-gal vector control (Fig. 7Ai,ii.). By contrast, at the same time-point, myotubes expressing all versions of mutant FHL1 (except RSS 151–153Δ) appeared to be smaller and contained fewer nuclei (Fig. 7Aiii,Bi; supplementary material Fig. S2A). Quantification of myotube area, length, width and fusion index revealed that myotubes expressing wild-type HA–FHL1 exhibited significantly increased myotube size and myonuclei number (i.e. fusion index) compared with those expressing the β-gal vector control (Fig. 7Bi,ii), consistent with previous findings (Cowling et al., 2008). By contrast, myotubes expressing the RBM, SPM and XMPMA mutants showed significantly reduced myotube size and myonuclei number compared with those expressing wild-type HA–FHL1 (Fig. 7Bi,ii, bars labelled ‘a’; see supplementary material Fig. S2 for full analysis).

We questioned whether the impaired myotube formation caused by these FHL1 mutants was due to the loss of normal FHL1 function, or to the gain of a dominant-negative or toxic function. If mutation leads to loss of normal FHL1 function, then myotube differentiation would be impaired relative to that of cells expressing wild-type HA–FHL1 but not cells expressing β-gal vector control. Alternatively, if mutation of FHL1 leads to gain of a dominant-negative or toxic function, then myotube differentiation might be reduced even relative to that of cells expressing β-gal vector control. Myotubes expressing SPM W122S and XMPMA 127-I-128 exhibited a reduced area and number of myonuclei compared with those expressing β-gal vector, indicating that FHL1 mutation might lead to both a loss of normal function and a gain of toxic function (Fig. 7Bi,ii, bars labelled ‘b’). Interestingly, impaired myotube differentiation was not observed in myotubes expressing FHL1 RSS 151–153Δ, and the expression of this mutant resulted in significantly larger myotubes compared with cells expressing β-gal vector control, similar to the effects of wild-type HA–FHL1. This suggests that aggregation per se does not induce loss of function. In all mutant-FHL1-expressing myoblasts no differences were observed in the proportion of cells that became myotubes (Fig. 7Biii) or in the ratio of cytoplasm to myonuclei (myonuclear domain) (supplementary material Fig. S2B), which normally remains constant during muscle remodelling (Allen et al., 1999). No differences were observed in the expression levels of MHC or myogenin protein throughout differentiation, as assessed by immunoblot analysis for FHL1 mutants (supplementary material Fig. S3).

We next correlated myoblast differentiation defects with the level of ectopic expression of RBM-associated C132F FHL1 mutant protein. If mutation only leads to loss of normal FHL1 function, then increased expression of mutant FHL1 should not further exacerbate myotube differentiation defects as the protein is non-functional. However, if mutation leads to the expression of a dominant-negative protein that opposes endogenous wild-type FHL1 function or leads to a gain of toxic function, then increased

Journal of Cell Science (2014) 127, 2269–2281 doi:10.1242/jcs.140905

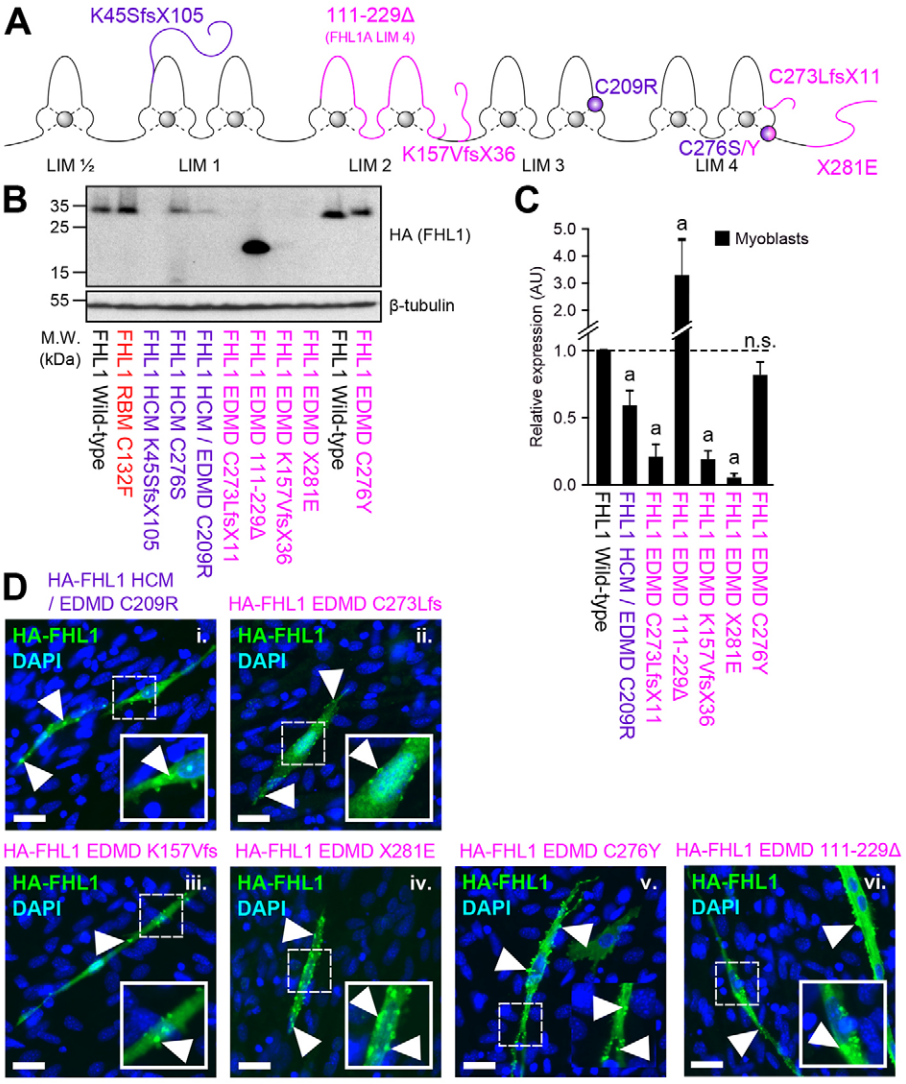

Fig. 6. FHL1 EDMD and HCM mutants exhibit altered expression and accumulate *in vitro*. (A) Diagram showing the FHL1 missense, frameshift and loss-of-stop-codon mutations identified in EDMD (pink) and HCM (purple) that are investigated here. These are; the previously reported HCM FHL1 K45SfsX105 and C276S mutations, EDMD FHL1 111–229delinsG (111–229Δ, predicted to replace LIM 2 with LIM 4), K157VfsX36, C276Y, C273LfsX11, X281E and HCM/EDMD FHL1C209R. (B) C2C12 myoblasts were transiently transfected with HA-tagged wild-type FHL1 or HCM or EDMD FHL1 mutants, and whole-cell lysates were immunoblotted with anti-HA and anti-β-tubulin antibodies after 48 hours of expression (myoblasts). (C) HA–FHL1 immunoblots were analysed by densitometry, quantified relative to the β-tubulin loading control and represented relative to wild-type HA–FHL1 (dashed black line). Data represent the mean±s.e.m.; $n=3$; $^{a}P<0.05$ compared with wild-type HA–FHL1; n.s., not significant. (D) Myotubes were differentiated for 72 hours, co-stained with anti-HA (green) and DAPI (nuclei, blue), and imaged by fluorescence wide-field microscopy. Inset, 2× magnification of dashed box; arrowheads, mutant HA–FHL1 accumulation. Scale bars: 50 μm.

expression of mutant FHL1 might further impair myotube formation in a dose-dependent manner. To this end, the relative fluorescence intensity of HA–FHL1 at 72 hours of differentiation was measured, each myotube was blindly categorised as having high, medium or low HA–FHL1 expression, and myotube area, length, width and fusion index were determined. Using this approach, myotubes expressing high levels of HA–FHL1 RBM C132F showed a significantly reduced area (~42%, $P<0.007$), number of myonuclei (~35%, $P<0.01$), length (~39%, $P<0.006$) and width (~25%, $P<0.02$) compared with myotubes expressing low levels of HA–FHL1 RBM C132F (Fig. 7C; data-points labelled ‘c’), indicative of a dose-dependent relationship. No differences in myonuclear domain were observed (supplementary material Fig. S2C). Myotubes expressing high levels of HA–FHL1 RBM C132F showed significantly reduced area (~40%; $P<0.008$) compared with those expressing high levels of wild-type HA–FHL1, and reductions in length, width and fusion index were also observed (Fig. 7C; data-points labelled ‘a’). Interestingly, myotubes with high expression of wild-type HA–FHL1 showed a trend towards reduced area, number of nuclei and length compared with cells with a low level of wild-type HA–FHL1 expression for unknown reasons, although this was not statistically significant.

Impaired myotube differentiation can be partially rescued by constitutively active NFATc1 but not wild-type NFATc1 or wild-type FHL1

NFATc1 is a transcription factor that, upon dephosphorylation by calcineurin, translocates to the nucleus to alter gene transcription. In skeletal muscle, NFATc1 activation leads to fibre-type switching and hypertrophy (Liu et al., 2001), and FHL1 directly binds to NFATc1 and enhances its transcriptional activity. Transgenic mice overexpressing FHL1 in skeletal muscle exhibit increased muscle-fibre size, dependent on calcineurin and NFAT, through increased expression of hypertrophic genes (such as GATA2) (Cowling et al., 2008). Aggregates of mutant FHL1 protein in RBM muscle colocalise with endogenous NFATc1 (Schessl et al., 2008), and aggregates of FHL1 sequester NFATc1 *in vitro* and reduce NFATc1 transcriptional activity (Cowling et al., 2008). Therefore, the myotube differentiation defects observed with FHL1 mutants might be mediated by reduced NFATc1 signalling as a consequence of its sequestration into aggregates. To address this possibility, we investigated whether increasing the expression of NFATc1 or wild-type FHL1 could rescue the formation of FHL1-mutant myotubes. As exogenous NFATc1 might also be sequestered within FHL1 aggregates, we also examined the effect of

Journal of Cell Science (2014) 127, 2269–2281 doi:10.1242/jcs.140905

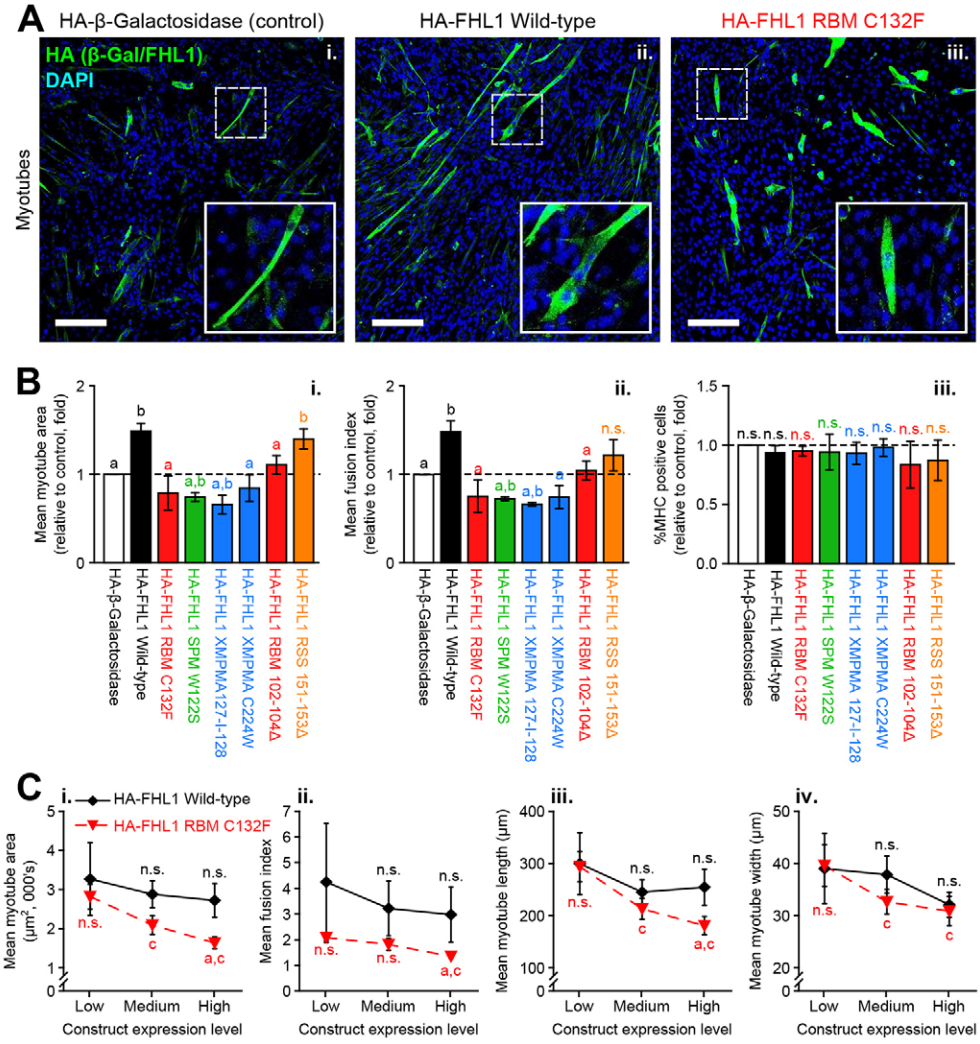

Fig. 7. FHL1 mutations cause loss of normal FHL1 function and impaired myotube formation. Myoblast differentiation was assessed in mutant-FHL1-expressing myotubes. C2C12 myoblasts were transiently transfected with the HA–FHL1 mutant RBM C132F, RBM 102–104Δ, SPM W122S, XMPMA 127-I-128, XMPMA C224W or RSS 151–153Δ, wild-type HA–FHL1 or β-galactosidase control, then differentiated for 72 hours. Cells were co-stained with anti-HA (FHL1, green), anti-myosin-heavy-chain (MHC, not shown) and DAPI (nuclei, blue), then imaged by large-tiled fluorescence confocal microscopy. (A) Representative fields of β-galactosidase control (i), wild-type HA–FHL1 (ii) or RBM C132F (iii). Inset, 2.5× magnification of dashed box. See supplementary material Fig. S2A for representative images of SPM, XMPMA and deletion mutants. Scale bars: 100 μm. (B) Transfected myotubes (cells positive for HA–FHL1 and MHC) were assessed for myotube area (i) and fusion index (ii) relative to β-galactosidase control (dashed black line). See supplementary material Fig. S2B for myonuclear domain, length and width. (iii) The percentage of transfected cells positive for MHC was similar between wild-type FHL1 (74%), FHL1 mutants (65–76%) and β-galactosidase control (78%). Data represent the mean±s.e.m.; ≥100 cells per independent experiment; $n \geq 3$; $^{a}P<0.05$ compared with wild-type HA–FHL1; $^{b}P<0.05$ compared with β-galactosidase control; n.s., not significant. (C) Dose-dependent impairment of differentiation in RBM C132F myotubes was determined by categorising myotubes into low (<15%), medium (15–60%) or high (>60%) HA–FHL1 expression, and myotube area (i), fusion index (ii), length (iii) and width (iv) were determined. Data represent the mean±s.e.m.; ≥100 cells per independent experiment; $n \geq 5$; $^{a}P<0.05$ compared with wild-type FHL1 at the same expression level; $^{c}P<0.05$ compared with low expression of the same construct; n.s., not significant (paired *t*-test).

constitutively active NFATc1 (CA-NFATc1), which contains mutations in the regulatory domain that prevent inhibitory phosphorylation of NFATc1 and thus render the protein constitutively nuclear and thereby active (Monticelli and Rao, 2002). C2C12 myoblasts were transfected with HA–FHL1 RBM C132F and co-transfected with wild-type GFP–NFATc1 (GFP–WT-NFATc1), constitutively active GFP–NFATc1 (GFP-CA-NFATc1) or Myc-tagged wild-type FHL1 (Myc–FHL1) (Fig. 8A). Differentiation was assessed after 72 hours as detailed above. Relative fluorescence intensity of HA–FHL1 was used to blindly categorise each myotube as having high, medium or low HA–FHL1 expression, and the relative fluorescence intensity of GFP or Myc was used to score high, medium or low rescue by GFP–NFATc1 or Myc–FHL1 expression. Coexpression of GFP–WT-NFATc1 at any expression level did not rescue impaired myotube formation in myotubes expressing high, medium or low levels of FHL1 RBM C132F (Fig. 8Ai,iv; supplementary material Fig. S4i–v). Notably, myotubes with low or medium expression of FHL1 RBM C132F and medium coexpression of CA-NFATc1 exhibited a ~25% increase in myotube area ($P<0.018$) and a ~23% increase in myonuclei number ($P<0.048$) compared with those with low CA-NFATc1 coexpression (Fig. 8Aii,v; supplementary material Fig. S4vi,vii.). In these myotubes, the mean myotube area was similar

Journal of Cell Science (2014) 127, 2269–2281 doi:10.1242/jcs.140905

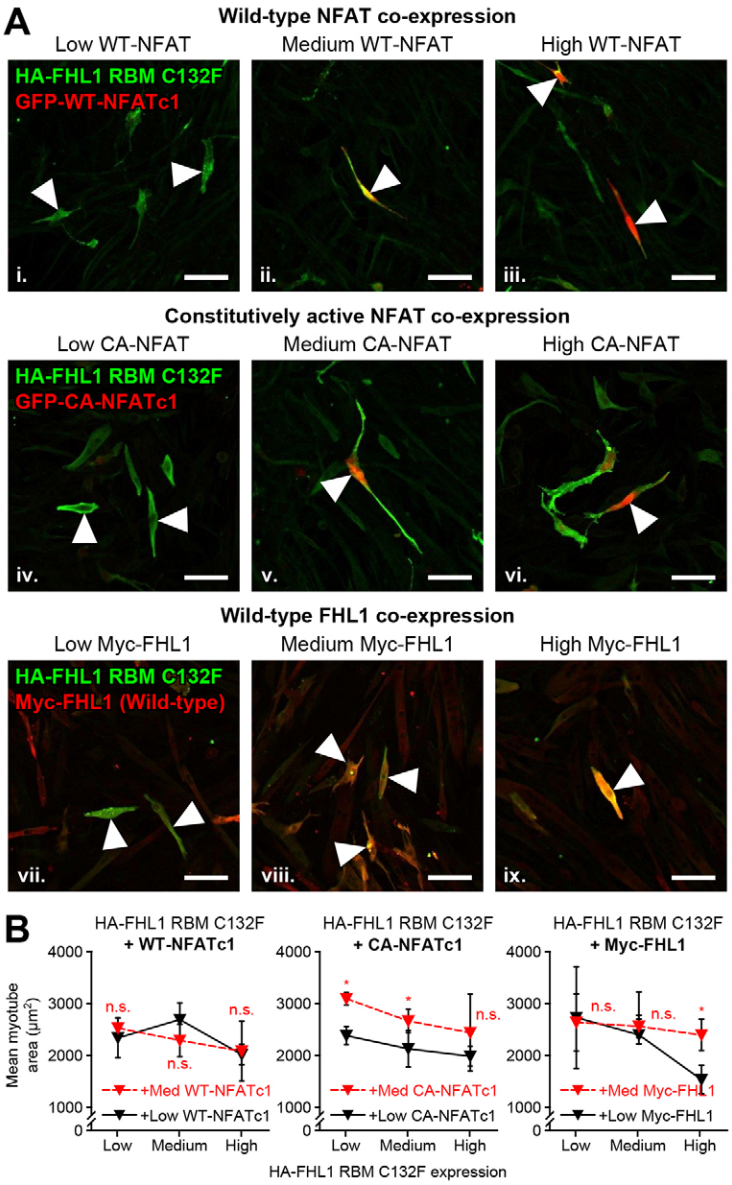

Fig. 8. Impaired myotube formation caused by FHL1 mutation can be rescued by constitutively active NFATc1. (A) C2C12 myoblasts were transiently transfected with HA–FHL1 RBM C132F and co-transfected with wild-type GFP–NFATc1, constitutively active GFP–NFATc1 or Myc–FHL1, then differentiated for 72 hours. Cells were co-stained with anti-HA (green), anti-myosin-heavy-chain (Alexa Fluor 647, not shown) and DAPI (blue), then imaged by large-tiled fluorescence confocal microscopy. Relative GFP–NFAT or Myc–FHL1 expression levels were determined by GFP fluorescence (red) or Myc staining (red). Myotubes were categorised into low (<15%), medium (15–60%) or high (>60%) HA–FHL1 expression, and low (<15%), medium (15–50%) or high (>50%) rescue expression (NFATc1 or Myc–FHL1), and the myotube area was assessed. Arrowheads, representative cells with the indicated rescue expression level. Scale bars: 100 μm. (B) Representative images show transfected cells with medium expression of HA–FHL1 RBM C132F and low, medium or high NFAT or FHL1 coexpression (arrowheads). See supplementary material Figs S4 and S5 for full analysis. Data represent the mean±s.e.m.; ≥50 cells per independent experiment; $n \geq 3$; *$P<0.05$ compared with low level expression of rescue at the same level of expression of HA–FHL1 RBM C132F; n.s., not significant (paired *t*-test).

to that observed in myotubes expressing wild-type HA–FHL1, as reported above (~3000 μm^2, Fig. 7Ci), indicating that GFP–CA-NFATc1 expression can rescue myoblast differentiation defects. Similar trends were observed for myotube length and width (supplementary material Fig. S4viii,ix), although not statistically significant, and no difference in myonuclear domain was observed. Interestingly, the increase in area and myonuclei number was less pronounced with high CA-NFATc1 coexpression, and was not statistically significant (supplementary material Fig. 4vi–x). Additionally, CA-NFATc1 coexpression did not rescue myotubes with high expression of FHL1 RBM C132F (as opposed to medium expression of FHL1 RBM C132F, which was rescued), and coexpression of CA-NFATc1 in myotubes expressing wild-type HA–FHL1 exhibited no significant effect on myotube differentiation (supplementary material Fig. 5vi–x).

Myc–WT-FHL1 overexpression did not increase myotube area in myotubes expressing low or medium levels of HA–FHL1 RBM C132F (Fig. 8Aiii,vi). Interestingly, only in myotubes expressing high HA–FHL1 RBM C132F was myotube area increased by medium Myc–WT-FHL1 coexpression compared with low Myc–WT-FHL1 coexpression. However, this effect might be attributed to a low level of Myc–WT-FHL1 coexpression causing reduced myotube area, as the myotube area appeared to be reduced in cells coexpressing a low level of Myc–WT-FHL1 compared with those coexpressing a low level of CA-NFAT (~1500 μm^2 versus ~2000 μm^2). Medium Myc–FHL1 expression might therefore only appear to rescue myotube area, as the myotube area is similar to that of cells with medium CA-NFAT coexpression, which did not rescue myotube area in myotubes expressing high HA–FHL1 RBM C132F (both ~2500 μm^2). Hence, it is uncertain whether wild-type FHL1 can rescue impaired myotube differentiation.

DISCUSSION

Recent studies have revealed that the gene *FHL1* is mutated in six different clinically defined human myopathies that exhibit a range of clinical features and disease severity. However, to date, the molecular basis of how *FHL1* mutation leads to myopathy remains unclear. In some cases, mutation leads to FHL1 protein

Journal of Cell Science (2014) 127, 2269–2281 doi:10.1242/jcs.140905

truncation associated with reduced protein expression, suggesting loss of function (Gueneau et al., 2009); however, in other cases, including the most severe clinical myopathies such as RBM, FHL1 expression remains at wild-type levels (Schessl et al., 2008; Shalaby et al., 2009). In RBM, mutant FHL1 is detected in intracellular proteinaceous aggregates that stain positively with M-NBT in the absence of substrate α-glycerophosphate (Brooke and Neville, 1972). These aggregates are termed 'reducing bodies' because they contain sulfhydryl compounds (Brooke and Neville, 1972), possibly owing to the accumulation of mutant FHL1 protein, which is rich in the sulfhydryl-group-containing amino acid cysteine. For other *FHL1* myopathies, such as SPM and XMPMA, clinically affected muscle was initially reported to contain desmin-positive cytoplasmic inclusions and vacuoles but not reducing bodies (Quinzii et al., 2008; Windpassinger et al., 2008). Therefore, whether these FHL1 mutants aggregate is unknown. Here, we report that SPM, XMPMA, RSS and RBM FHL1 mutants show similar recombinant protein expression levels to wild-type HA–FHL1 upon ectopic expression in C2C12 cells and also form protein aggregates that stain positively for the reducing body marker M-NBT, analogous to RBM FHL1 mutants. By contrast, HCM and EDMD FHL1 mutants exhibited reduced recombinant protein expression, except for one EDMD mutant that showed increased expression (111–229Δ), and all EDMD and HCM mutants appeared to accumulate *in vitro*. RBM, SPM and XMPMA, but not RSS mutants, exhibit reduced C2C12 myoblast fusion and differentiation relative to wild-type HA–FHL1, possibly due to loss of function. Notably, SPM W122S and XMPMA 127-I-128 FHL1 mutants also impaired myotube formation relative to vector control, and FHL1 RBM C132F showed a dose-dependent impairment of myoblast differentiation, suggesting that, in addition to loss of wild-type FHL1 function, a dominant-negative or gain of toxic function might occur. To dissect the possible mechanisms by which the loss of FHL1 function reduces myotube formation, we determined whether expression of wild-type FHL1 or its binding partner NFATc1, a known mediator of myoblast fusion (Semsarian et al., 1999), could rescue the mutant-FHL1 phenotype in C2C12 cells. Notably, neither wild-type FHL1 nor wild-type NFATc1 rescued mutant-FHL1-induced myoblast fusion defects, consistent with the contention that these FHL1 mutants might induce a gain of toxic function. Interestingly, expression of constitutively active NFAT partially restored myoblast fusion and myotube formation in cells expressing RBM-associated FHL1 mutants, suggesting that toxic function can, at least in part, be bypassed. Collectively, this study reveals that several clinically distinct FHL1-associated myopathies, including RBM, SPM and XMPMA, might involve common molecular events, including FHL1-mutant aggregation, loss of normal function and potentially dominant-negative function or gain of toxic function.

FHL1 protein is expressed at reduced, normal or elevated levels in RBM patient muscle (Schessl et al., 2008; Shalaby et al., 2009; Schreckenbach et al., 2013) (supplementary material Table S1). By contrast, SPM muscle exhibits absent, reduced or normal levels of FHL1 protein expression (Quinzii et al., 2008), and FHL1 is absent from XMPMA-afflicted muscle, as assessed by FHL1 immunoblot analysis (Windpassinger et al., 2008; Schoser et al., 2009). We demonstrate here, using ectopic expression in C2C12 cells, that RBM, SPM, XMPMA and RSS mutant FHL1 protein expression is equivalent to wild-type HA–FHL1 expression *in vitro* in myoblasts and in myotubes for up to 72 hours. It is possible that the available FHL1 antibodies used in clinical studies might not recognise mutated FHL1 protein, particularly that containing frameshift mutations and mutations that affect the recognised epitope (a problem avoided here *in vitro* by N-terminal HA tagging of FHL1 mutants), and/or aggregated endogenous FHL1 might not be readily detected owing to protein insolubility (avoided here by analysing whole-cell lysates). Indeed, XMPMA muscle biopsies and isolated myoblasts exhibit endogenous mutant FHL1 expression (albeit reduced) as assessed by immunohistochemistry (Windpassinger et al., 2008), but western blot analysis of XMPMA muscle exhibits no mutant FHL1 protein expression (Windpassinger et al., 2008; Schoser et al., 2009). Interestingly, we have reported recently that ectopic expression of FHL1 frameshift and premature stop mutations that were identified in HCM leads to the degradation of truncated mutant FHL1 protein in C2C12 myoblasts, which can be rescued by inhibition of the proteasome (Friedrich et al., 2012). Here, we show that EDMD FHL1 and another HCM/EDMD FHL1 mutant exhibit reduced expression; however, another EDMD FHL1 mutant exhibits increased expression. Therefore, the capacity for mutant FHL1 to be degraded by the proteasome/ubiquitin pathway or by mutant aggregate clearance might be dependent on the nature and/or location of the FHL1 mutation. The apparent absence of mutant FHL1 protein expression or aggregates in some biopsied muscle from affected individuals might be a consequence of the patchy nature of the muscle disease and/or the stage of disease progression at the time of biopsy.

Many clinical symptoms of RBM overlap with those of SPM and XMPMA, including severely affected males and variable penetrance in females, spinal rigidity, scapular winging, contractures and cardiac involvement (Cowling et al., 2011). Benign cases of RBM have a very low prevalence of reducing bodies, between 0.2 and 0.5% of biopsied muscle fibres (Tomé and Fardeau, 1975; Oh et al., 1983), and inclusion prevalence varies between muscle fascicles (Schreckenbach et al., 2013). It is interesting to speculate that SPM and XMPMA might represent a continuum of benign RBM with a low abundance of reducing bodies that are difficult to detect or are cleared in affected muscle biopsies. In a recent publication, a personal communication reported that re-examined SPM tissue was positive for reducing bodies; however, supporting data was not shown (Schessl et al., 2009). 'Cytoplasmic bodies' and 'atypical reducing bodies' were originally observed in XMPMA (Schoser et al., 2009), and recent reports have revealed that reducing bodies and protein aggregation might occur in XMPMA muscle (Feldkirchner et al., 2011; Feldkirchner et al., 2013). Additionally, cytoplasmic bodies have been observed in a skeletal-muscle biopsy taken from a HCM/EDMD patient with the FHL1 C209R mutation that was investigated here (Knoblauch et al., 2010). Here, we demonstrate that RBM, RSS, SPM and XMPMA mutants aggregate *in vitro* in C2C12 cells. However, we cannot exclude the possibility that the ectopic expression system used in our cell culture model expresses mutant proteins at higher levels than those that occur *in vivo* and this might contribute to a propensity to aggregate; however, this was not observed for the wild–type FHL1, suggesting that this is an intrinsic propensity of these mutant FHL1 proteins. All RBM, SPM and XMPMA FHL1 mutants colocalised with ubiquitin staining in C2C12 cells, suggesting that mutant FHL1 might be targeted for degradation by the ubiquitin proteasome system. As shown here in myotubes expressing RBM, SPM and XMPMA mutant FHL1, the proportion of cells that contained aggregates increased over time *in vitro*, possibly reflecting the observed accumulation of aggregates over time in RBM patient muscle (Schessl et al.,

2009). The phenotypically milder deletion mutants RBM 102–104Δ and RSS 151–153Δ exhibited similar expression to that of wild-type HA–FHL1 and also formed aggregates. Additionally, the clinical presentation of the RSS FHL1 three-amino-acid-deletion mutant is analogous to that of RBM patients, and this FHL1 mutant similarly formed aggregates both in patient muscle (Shalaby et al., 2008) and here *in vitro*; therefore, the FHL1 RSS 151–153Δ mutant might be associated with a continuum of RBM with a clinically milder syndrome for unknown reasons.

Whether FHL1 mutations result in myopathy due to loss of normal FHL1 function has not been reported to date. FHL1 increases fibre size and myoblast fusion through enhanced calcineurin–NFATc1 signalling (Cowling et al., 2008). NFATc1 is dephosphorylated by calcineurin, allowing its translocation to the nucleus to enhance transcription of hypertrophy-inducing genes, which is enhanced by FHL1 (Cowling et al., 2008), leading to fibre-type switching and hypertrophy (Liu et al., 2001). Myoblast fusion is an essential step in muscle growth during development and for the regeneration of mature muscle (Pavlath and Horsley, 2003). Impaired myoblast fusion is observed in several myopathies (de Luna et al., 2006; Merrick et al., 2009; Vesa et al., 2009). Relative to wild-type HA–FHL1, which enhanced myoblast differentiation, the expression of RBM, SPM or XMPMA mutant HA–FHL1 did not promote increased myoblast fusion and myotube size *in vitro*. Myoblasts isolated from two EDMD patients harbouring the X281E and K157VfsX46 mutations investigated here exhibit reduced expression of mutant FHL1 and delayed myoblast differentiation (Gueneau et al., 2009). Similarly, shRNA-mediated knock-down of FHL1 impairs myotube formation *in vitro* (Lee et al., 2012). FHL1 expression is decreased in animal models of disuse atrophy (Loughna et al., 2000), and FHL1 protein expression might be reduced in SPM, XMPMA and RSS, which might further exacerbate the loss of normal FHL1 function caused by mutation. *Fhl1*-null mice were initially reported to exhibit normal life spans and no gross skeletal-muscle defects (Chu et al., 2000; Kudo et al., 2007; Sheikh et al., 2008), although a recent report describes a lethal age-dependant severe myopathy (Domenighetti et al., 2014). SPM, XMPMA and benign RBM cases exhibit adult onset rather than a developmental defect, suggesting that loss of FHL1 function alone might be insufficient to cause severe disease.

FHL1 mutations might cause a dominant-negative function or lead to the gain of a new toxic function. Here, we report that expression of SPM W122S and XMPMA 127-I-128 mutant FHL1 protein impairs myoblast differentiation compared with expression of the β-galactosidase control, indicating these FHL1 mutants have a more negative influence on myotube formation than would be expected from the loss of normal FHL1 function alone. We also show dose-dependent toxicity, where myotubes with higher expression of FHL1 RBM C132F exhibit reduced myotube size and fusion compared with those showing low FHL1 RBM C132F expression. This is consistent with the generally observed X-linked dominant clinical features of RBM, SPM and XMPMA (Quinzii et al., 2008; Schessl et al., 2008; Windpassinger et al., 2008). Additionally, coexpression of wild-type Myc–FHL1 is unable to rescue impaired myotube formation in cells expressing FHL1 RBM C132F, indicating that FHL1 mutation and aggregate formation confers a dominant-negative function or gain of a new toxic function. Only constitutively active NFATc1 could increase myotube size and fusion in myotubes expressing FHL1 RBM C132F; however, this was only observed in cells with low to medium expression of mutant FHL1.

Protein aggregates are implicated in many neurological disorders, including Alzheimer's, Parkinson's and Huntington's diseases (Ross and Poirier, 2004), and muscular disorders, including myofibrillar myopathy (Schröder and Schoser, 2009), inclusion body myositis (Dalakas, 2006) and oculopharyngeal muscular dystrophy (Brais et al., 1998). Growing evidence suggests that aggregate precursors and the cellular response they elicit causes cellular toxicity (reviewed in Stefani and Dobson, 2003), and that the formation of aggresomes might be cytoprotective (Tanaka et al., 2004). Inhibition of aggresome formation in a model of spinobulbar muscular atrophy (SBMA) increases cellular cytotoxicity *in vitro* (Taylor et al., 2003). Reducing bodies observed in RBM patients resemble aggresomes (Liewluck et al., 2007), and we show here that aggregates of RBM, SPM and XMPMA mutant FHL1 co-stained with GRP78, a marker of aggresomes that binds to misfolded proteins and activates the UPR. Sustained activation of the UPR causes toxicity *in vitro* (Thomas et al., 2005) and neurodegeneration in a mouse prion model (Moreno et al., 2012). Significantly, neurodegeneration can be prevented by restoring the cell translational machinery that is blocked by UPR signalling, even though protein aggregation remains unchanged (Moreno et al., 2012). By contrast, inhibiting aggregation of tau or polyglutamine protein failed to prevent neurotoxicity in a zebrafish model of Alzheimer's disease (van Bebber et al., 2010). It remains unclear what role the UPR plays in *FHL1* myopathies. We report that the FHL1 RSS 151–153Δ mutant exhibits FHL1 aggregation and formation of reducing bodies, yet, surprisingly, myotube formation was comparable to that of cells expressing wild-type HA–FHL1. This suggests that aggregates per se might not cause toxicity, and it is unclear whether different FHL1 mutants generate different pre-fibrillar species that confer varied toxicity. Taken together, this suggests that targeting the gain of toxic function rather than preventing FHL1 aggregation might have therapeutic potential for *FHL1* myopathies.

In summary, our study suggests that RBM, SPM and XMPMA share a common pathogenesis, whereby mutant FHL1 accumulates in reducing bodies. Mutant FHL1 expression is maintained *in vitro*; however, the normal function of enhancing myoblast size and fusion is lost. Furthermore, mutant FHL1 expression dominantly impairs myotube formation, which could not be rescued by wild-type FHL1 or NFATc1, suggesting that potential therapeutics should target the gain of new toxic function or mechanisms that enhance myoblast fusion.

MATERIALS AND METHODS

Constructs

pCGN-FHL1 (human cDNA, GenBank/EMBL/DDBJ accession number NM_001449), pCGN-β-galactosidase (vector control) and the RBM FHL1 mutants C132F and H123Y have been described previously (Cowling et al., 2008). To generate RBM, SPM, XMPMA, RSS, CM and EDMD mutants, pCGN wild-type FHL1 was used as a template for site-directed mutagenesis (see supplementary material Table S2 for primers), and 5′ *Xba*I and 3′ *Xma*I sites were introduced. These fragments were cloned into pCR-Blunt before *Xba*I and *Xma*I digestion and directional ligation back into the pCGN mammalian expression vector. pGEM-T FHL1 EDMD X281E was a gift from G.B. and was re-cloned into pCGN. WT-NFATc1 (NFAT2; Addgene plasmid 11101) and CA-NFATc1 (Addgene plasmid 11102) were obtained from Addgene (Cambridge, MA) (Monticelli and Rao, 2002).

Reagents

Reagents were obtained as follows: C2C12 myoblasts were from the American Type Culture Collection (Manassas, VA); fibronectin (F1141), DAPI (D9542), Menadione (M5625), NBT (N6639), L-glutamine (G7513),

penicillin-streptomycin (P4333), trypsin (T4049), MG132 (C2211) and bafilomycin-A1 (B1793) were from Sigma-Aldrich (Sydney, Australia); Optimem (22600050), Lipofectamine 2000 (11668019), fetal bovine serum (FBS, 10099141), horse serum (16050122), DMEM (12500062), SlowFade Gold (S36936) and Zero Blunt TOPO (K275020) were from Life Technologies Australia (Mulgrave, Australia).

Antibodies

The primary antibodies used were: mouse anti-HA (MMS101P) from Covance (North Ryde, Australia); goat-anti HA (ab9134) and rabbit anti-ubiquitin (ab7780) from Abcam (Cambridge, UK); mouse anti-NFATc1 (sc7294) and anti-myogenin (sc576) from Santa Cruz Antibodies (Santa Cruz, CA); rabbit anti-myc (2278) from Cell Signalling Technology (Beverly, MA); rabbit anti-GRP78/BiP (G8918) from Sigma-Aldrich; mouse anti-GFP (11814460001) from Roche (Hawthorn, Australia); and mouse β-tubulin (322600) from Life Technologies Australia. The sarcomeric MyHC mouse antibody (MF20) was obtained from the Developmental Studies Hybridoma Bank, developed under the auspices of the National Institutes of Health and maintained by the Department of Biological Sciences, University of Iowa (Bader et al., 1982). Secondary antibodies were as follows: anti-mouse or anti-rabbit conjugated with HRP were obtained from Merck Millipore (Kilsyth, Australia); and all Alexa-Fluor-conjugated secondary antibodies were from Life Technologies.

Growth, differentiation, transient transfection and immunohistochemistry of C2C12 cells

C2C12 myoblasts were passaged subconfluently in DMEM supplemented with 20% FBS, 2 mM L-glutamine and penicillin-streptomycin. C2C12 differentiation was performed as described previously (Cowling et al., 2008). Briefly, 10^5 myoblasts were plated onto fibronectin-coated coverslips (5 µg/ml) for 24 hours, then transiently transfected with 10 µg of total DNA with Lipofectamine 2000 in OptiMem medium as per the manufacturer's instructions. After 4 hours, the cells were returned to growth medium, then after 24 hours the cells were induced to differentiate to myotubes for 0–120 hours in medium containing 5% horse serum. Cells were then fixed, permeabilised, blocked and stained with the appropriate nuclear stains, antibodies and/or Menadione-NBT, as described previously (McGrath et al., 2003; McGrath et al., 2006; Cowling et al., 2008). For western blot analysis, whole-cell lysates were prepared in SDS-PAGE reducing buffer (Laemmli) and 25 µl of lysates were immunoblotted with antibodies against HA (1:5000), GFP (1:1000), myogenin (1:500), MyHC (1:500) and β-tubulin (1:5000) as described previously (Cowling et al., 2008). For MG132 and bafilomycin treatments, cells were transfected as above, then after 24 hours the cells were treated for 24 hours in growth medium with 20 µM MG132 in 0.1% DMSO, 5 nM bafilomycin-A1 in 0.1% DMSO or with vehicle alone.

C2C12 differentiation analysis

Myoblast differentiation was assessed by measuring myotube area, length, width, fusion index and myonuclear domain. Briefly, transiently transfected myoblasts were differentiated for 72 hours, then stained as above. A 10×10 tiled image of each coverslip was analysed using ImageJ. At least 50 (average $n=76$) individual transfected cells (as determined by HA fluorescence) for each transfection condition and replicate were manually traced using the Versatile Wand Tool and polygon tools. For each traced cell, HA–FHL1 fluorescence was automatically measured (mean intensity), the area was automatically measured, total myonuclei were counted by DAPI staining and MyHC fluorescence was used to identify myotubes. The maximum Feret length and minimum Feret length were automatically measured to determine myotube length and width, respectively. For each replicate experiment, cells were categorised into low (<15%), medium (15–60%) or high (>60%) HA–FHL1 expression based on HA–FHL1 fluorescence intensity relative to cells within the same coverslip, thereby enabling differentiation measurements to be represented relative to the level of HA–FHL1 expression (dose-dependence) and acting as an internal control, as cells within the transfection or coverslip were compared.

C2C12 differentiation rescue experiments

For GFP–NFAT and Myc-FHL1 rescue experiments, cells were transfected as above using 5 µg of HA–FHL1 and 5 µg of GFP–NFATc1 or Myc–FHL1. Cell differentiation was analysed as above. GFP fluorescence or Myc staining was blindly and automatically measured for each traced cell to categorise each cell into low (<15%), medium (15–50%) or high (>50%) rescue expression relative to cells within the same coverslip.

Image and statistical analysis

All microscopy was performed at Monash Micro Imaging (MMI) at Monash University, Australia. All samples for microscopy were mounted in SlowFade Gold reagent and viewed at room temperature. Confocal fluorescence microscopy was performed using a Nikon Upright C1 confocal laser scanning microscope. Nikon Imaging Software (NIS-elements) was used for confocal image acquisition. Fluorescence and light microscopy was performed using a microscope (AX70 Provis; Olympus) fitted with either a charge-coupled device (colour; DP70; Olympus) or FVII monochrome (black and white; Olympus) camera. AnalySiS software was used for image capture. High resolution confocal *z*-stacks were imaged and analysed in Imaris to generate surface renderings of mutant FHL1 accumulations.

Western blot films were scanned and band signal intensities were determined using ImageJ (Schneider et al., 2012) (Analyse→Gel tools). Densitometry values were expressed as a fold difference relative to the control, standardised to corresponding total β-tubulin values. All results are presented as the mean±s.e.m. Statistical analysis was performed in LibreOffice Calc spreadsheet using the unpaired two-tailed Student's *t*-test unless stated otherwise. *P*-values of <0.05 were considered statistically significant.

Acknowledgements

We thank Silvia Monticelli (Monticelli and Rao, 2002) for NFATc1 (NFAT2) plasmids, Esma Ziat (Inserm, Paris, France) for the pGEM-T FHL1 EDMD X281E cloning plasmid, and Rajendra Gurung (Monash University, Clayton, Australia) and Absorn Sriratana (Monash University, Clayton, Australia) for help with cloning. We also thank Monash Micro Imaging.

Competing interests

The authors declare no competing interests.

Author contributions

C.A.M., M.J.M. and B.R.W. designed the study; B.R.W. performed experiments and prepared the manuscript; C.A.M., M.J.M. and G.B. edited the manuscript.

Funding

This work was supported by the Australian National Health and Medical Research Council [grant number 1010655 to C.A.M. and M.J.M.] and an Australian Postgraduate Award Scholarship to B.R.W.

Supplementary material

Supplementary material available online at
http://jcs.biologists.org/lookup/suppl/doi:10.1242/jcs.140905/-/DC1

References

Allen, D. L., Roy, R. R. and Edgerton, V. R. (1999). Myonuclear domains in muscle adaptation and disease. *Muscle Nerve* **22**, 1350-1360.

Bader, D., Masaki, T. and Fischman, D. A. (1982). Immunochemical analysis of myosin heavy chain during avian myogenesis in vivo and in vitro. *J. Cell Biol.* **95**, 763-770.

Brais, B., Bouchard, J. P., Xie, Y. G., Rochefort, D. L., Chrétien, N., Tomé, F. M., Lafrenière, R. G., Rommens, J. M., Uyama, E., Nohira, O. et al. (1998). Short GCG expansions in the PABP2 gene cause oculopharyngeal muscular dystrophy. *Nat. Genet.* **18**, 164-167.

Brooke, M. H. and Neville, H. E. (1972). Reducing body myopathy. *Neurology* **22**, 829-840.

Brown, S., Biben, C., Ooms, L. M., Maimone, M., McGrath, M. J., Gurung, R., Harvey, R. P. and Mitchell, C. A. (1999). The cardiac expression of striated muscle LIM protein 1 (SLIM1) is restricted to the outflow tract of the developing heart. *J. Mol. Cell. Cardiol.* **31**, 837-843.

Chen, D. H., Raskind, W. H., Parson, W. W., Sonnen, J. A., Vu, T., Zheng, Y., Matsushita, M., Wolff, J., Lipe, H. and Bird, T. D. (2010). A novel mutation in FHL1 in a family with X-linked scapuloperoneal myopathy: phenotypic spectrum and structural study of FHL1 mutations. *J. Neurol. Sci.* **296**, 22-29.

Journal of Cell Science

Chu, P. H., Ruiz-Lozano, P., Zhou, Q., Cai, C. and Chen, J. (2000). Expression patterns of FHL/SLIM family members suggest important functional roles in skeletal muscle and cardiovascular system. *Mech. Dev.* **95**, 259-265.
Cowling, B. S., McGrath, M. J., Nguyen, M. A., Cottle, D. L., Kee, A. J., Brown, S., Schessl, J., Zou, Y., Joya, J., Bönnemann, C. G. et al. (2008). Identification of FHL1 as a regulator of skeletal muscle mass: implications for human myopathy. *J. Cell Biol.* **183**, 1033-1048.
Cowling, B. S., Cottle, D. L., Wilding, B. R., D'Arcy, C. E., Mitchell, C. A. and McGrath, M. J. (2011). Four and a half LIM protein 1 gene mutations cause four distinct human myopathies: a comprehensive review of the clinical, histological and pathological features. *Neuromuscul. Disord.* **21**, 237-251.
Dalakas, M. C. (2006). Sporadic inclusion body myositis – diagnosis, pathogenesis and therapeutic strategies. *Nat. Clin. Pract. Neurol.* **2**, 437-447.
de Luna, N., Gallardo, E., Soriano, M., Dominguez-Perles, R., de la Torre, C., Rojas-García, R., García-Verdugo, J. M. and Illa, I. (2006). Absence of dysferlin alters myogenin expression and delays human muscle differentiation ''in vitro''. *J. Biol. Chem.* **281**, 17092-17098.
Domenighetti, A. A., Chu, P. H., Wu, T., Sheikh, F., Gokhin, D. S., Guo, L. T., Cui, Z., Peter, A. K., Christodoulou, D. C., Parfenov, M. G. et al. (2014). Loss of FHL1 induces an age-dependent skeletal muscle myopathy associated with myofibrillar and intermyofibrillar disorganization in mice. *Hum. Mol. Genet.* **23**, 209-225.
Feldkirchner, S., Walter, M. C., Kubny, C., Mueller, S., Kress, W., Hanisch, F. G., Schoser, B. and Schessl, J. (2011). P5.53 The C224W FHL1 mutation is causing a protein aggregation disorder of muscle: Two brothers revisited. *Neuromuscul. Disord.* **21**, 740.
Feldkirchner, S., Walter, M. C., Müller, S., Kubny, C., Krause, S., Kress, W., Hanisch, F. G., Schoser, B. and Schessl, J. (2013). Proteomic characterization of aggregate components in an intrafamilial variable FHL1-associated myopathy. by a novel mutation in four-and-a-half LIM domain 1 gene (FHL1). *Neuromuscul. Disord.* **23**, 418-426.
Friedrich, F. W., Wilding, B. R., Reischmann, S., Crocini, C., Lang, P., Charron, P., Müller, O. J., McGrath, M. J., Vollert, I., Hansen, A. et al. (2012). Evidence for FHL1 as a novel disease gene for isolated hypertrophic cardiomyopathy. *Hum. Mol. Genet.* **21**, 3237-3254.
Greene, W. K., Baker, E., Rabbitts, T. H. and Kees, U. R. (1999). Genomic structure, tissue expression and chromosomal location of the LIM-only gene, SLIM1. *Gene* **232**, 203-207.
Gueneau, L., Bertrand, A. T., Jais, J. P., Salih, M. A., Stojkovic, T., Wehnert, M., Hoeltzenbein, M., Spuler, S., Saitoh, S., Verschueren, A. et al. (2009). Mutations of the FHL1 gene cause Emery-Dreifuss muscular dystrophy. *Am. J. Hum. Genet.* **85**, 338-353.
Knoblauch, H., Geier, C., Adams, S., Budde, B., Rudolph, A., Zacharias, U., Schulz-Menger, J., Spuler, A., Yaou, R. B., Nürnberg, P. et al. (2010). Contractures and hypertrophic cardiomyopathy in a novel FHL1 mutation. *Ann. Neurol.* **67**, 136-140.
Kopito, R. R. (2000). Aggresomes, inclusion bodies and protein aggregation. *Trends Cell Biol.* **10**, 524-530.
Kudo, L. C., Karsten, S. L., Chen, J., Levitt, P. and Geschwind, D. H. (2007). Genetic analysis of anterior posterior expression gradients in the developing mammalian forebrain. *Cereb. Cortex* **17**, 2108-2122.
Lee, S. M., Tsui, S. K., Chan, K. K., Garcia-Barcelo, M., Waye, M. M., Fung, K. P., Liew, C. C. and Lee, C. Y. (1998). Chromosomal mapping, tissue distribution and cDNA sequence of four-and-a-half LIM domain protein 1 (FHL1). *Gene* **216**, 163-170.
Lee, J. Y., Chien, I. C., Lin, W. Y., Wu, S. M., Wei, B. H., Lee, Y. E. and Lee, H. H. (2012). Fhl1 as a downstream target of Wnt signaling to promote myogenesis of C2C12 cells. *Mol. Cell. Biochem.* **365**, 251-262.
Liewluck, T., Hayashi, Y. K., Ohsawa, M., Kurokawa, R., Fujita, M., Noguchi, S., Nonaka, I. and Nishino, I. (2007). Unfolded protein response and aggresome formation in hereditary reducing-body myopathy. *Muscle Nerve* **35**, 322-326.
Liu, Y., Cseresnyés, Z., Randall, W. R. and Schneider, M. F. (2001). Activity-dependent nuclear translocation and intranuclear distribution of NFATc in adult skeletal muscle fibers. *J. Cell Biol.* **155**, 27-40.
Loughna, P. T., Mason, P., Bayol, S. and Brownson, C. (2000). The LIM-domain protein FHL1 (SLIM 1) exhibits functional regulation in skeletal muscle. *Mol. Cell Biol. Res. Commun.* **3**, 136-140.
McGrath, M. J., Mitchell, C. A., Coghill, I. D., Robinson, P. A. and Brown, S. (2003). Skeletal muscle LIM protein 1 (SLIM1/FHL1) induces alpha 5 beta 1-integrin-dependent myocyte elongation. *Am. J. Physiol.* **285**, C1513-C1526.
McGrath, M. J., Cottle, D. L., Nguyen, M. A., Dyson, J. M., Coghill, I. D., Robinson, P. A., Holdsworth, M., Cowling, B. S., Hardeman, E. C., Mitchell, C. A. et al. (2006). Four and a half LIM protein 1 binds myosin-binding protein C and regulates myosin filament formation and sarcomere assembly. *J. Biol. Chem.* **281**, 7666-7683.
Merrick, D., Stadler, L. K., Larner, D. and Smith, J. (2009). Muscular dystrophy begins early in embryonic development deriving from stem cell loss and disrupted skeletal muscle formation. *Dis. Model. Mech.* **2**, 374-388.
Monticelli, S. and Rao, A. (2002). NFAT1 and NFAT2 are positive regulators of IL-4 gene transcription. *Eur. J. Immunol.* **32**, 2971-2978.
Moreno, J. A., Radford, H., Peretti, D., Steinert, J. R., Verity, N., Martin, M. G., Halliday, M., Morgan, J., Dinsdale, D., Ortori, C. A. et al. (2012). Sustained translational repression by eIF2α-P mediates prion neurodegeneration. *Nature* **485**, 507-511.
Morgan, M. J. and Madgwick, A. J. (1999). The LIM proteins FHL1 and FHL3 are expressed differently in skeletal muscle. *Biochem. Biophys. Res. Commun.* **255**, 245-250.
Oh, S. J., Meyers, G. J., Wilson, E. R., Jr and Alexander, C. B. (1983). A benign form of reducing body myopathy. *Muscle Nerve* **6**, 278-282.
Pavlath, G. K. and Horsley, V. (2003). Cell fusion in skeletal muscle—central role of NFATC2 in regulating muscle cell size. *Cell Cycle* **2**, 419-422.
Quinzii, C. M., Vu, T. H., Min, K. C., Tanji, K., Barral, S., Grewal, R. P., Kattah, A., Camaño, P., Otaegui, D., Kunimatsu, T. et al. (2008). X-linked dominant scapuloperoneal myopathy is due to a mutation in the gene encoding four-and-a-half-LIM protein 1. *Am. J. Hum. Genet.* **82**, 208-213.
Ross, C. A. and Poirier, M. A. (2004). Protein aggregation and neurodegenerative disease. *Nat. Med.* **10 Suppl.**, S10-S17.
Schessl, J., Zou, Y., McGrath, M. J., Cowling, B. S., Maiti, B., Chin, S. S., Sewry, C., Battini, R., Hu, Y., Cottle, D. L. et al. (2008). Proteomic identification of FHL1 as the protein mutated in human reducing body myopathy. *J. Clin. Invest.* **118**, 904-912.
Schessl, J., Taratuto, A. L., Sewry, C., Battini, R., Chin, S. S., Maiti, B., Dubrovsky, A. L., Erro, M. G., Espada, G., Robertella, M. et al. (2009). Clinical, histological and genetic characterization of reducing body myopathy caused by mutations in FHL1. *Brain* **132**, 452-464.
Schessl, J., Columbus, A., Hu, Y., Zou, Y., Voit, T., Goebel, H. H. and Bönnemann, C. G. (2010). Familial reducing body myopathy with cytoplasmic bodies and rigid spine revisited: identification of a second LIM domain mutation in FHL1. *Neuropediatrics* **41**, 43-46.
Schmeichel, K. L. and Beckerle, M. C. (1997). Molecular dissection of a LIM domain. *Mol. Biol. Cell* **8**, 219-230.
Schneider, C. A., Rasband, W. S. and Eliceiri, K. W. (2012). NIH Image to ImageJ: 25 years of image analysis. *Nat. Methods* **9**, 671-675.
Schoser, B., Goebel, H. H., Janisch, I., Quasthoff, S., Rother, J., Bergmann, M., Müller-Felber, W. and Windpassinger, C. (2009). Consequences of mutations within the C terminus of the FHL1 gene. *Neurology* **73**, 543-551.
Schreckenbach, T., Henn, W., Kress, W., Roos, A., Maschke, M., Feiden, W., Dillmann, U., Schulz, J. B., Weis, J. and Claeys, K. G. (2013). Novel FHL1 mutation in a family with reducing body myopathy. *Muscle Nerve* **47**, 127-134.
Schröder, R. and Schoser, B. (2009). Myofibrillar myopathies: a clinical and myopathological guide. *Brain Pathol.* **19**, 483-492.
Selcen, D., Bromberg, M. B., Chin, S. S. and Engel, A. G. (2011). Reducing bodies and myofibrillar myopathy features in FHL1 muscular dystrophy. *Neurology* **77**, 1951-1959.
Semsarian, C., Wu, M. J., Ju, Y. K., Marciniec, T., Yeoh, T., Allen, D. G., Harvey, R. P. and Graham, R. M. (1999). Skeletal muscle hypertrophy is mediated by a Ca2+-dependent calcineurin signalling pathway. *Nature* **400**, 576-581.
Shalaby, S., Hayashi, Y. K., Goto, K., Ogawa, M., Nonaka, I., Noguchi, S. and Nishino, I. (2008). Rigid spine syndrome caused by a novel mutation in four-and-a-half LIM domain 1 gene (FHL1). *Neuromuscul. Disord.* **18**, 959-961.
Shalaby, S., Hayashi, Y. K., Nonaka, I., Noguchi, S. and Nishino, I. (2009). Novel FHL1 mutations in fatal and benign reducing body myopathy. *Neurology* **72**, 375-376.
Sheikh, F., Raskin, A., Chu, P. H., Lange, S., Domenighetti, A. A., Zheng, M., Liang, X., Zhang, T., Yajima, T., Gu, Y. et al. (2008). An FHL1-containing complex within the cardiomyocyte sarcomere mediates hypertrophic biomechanical stress responses in mice. *J. Clin. Invest.* **118**, 3870-3880.
Stefani, M. and Dobson, C. M. (2003). Protein aggregation and aggregate toxicity: new insights into protein folding, misfolding diseases and biological evolution. *J Mol Med (Berl)* **81**, 678-699.
Tanaka, M., Kim, Y. M., Lee, G., Junn, E., Iwatsubo, T. and Mouradian, M. M. (2004). Aggresomes formed by alpha-synuclein and synphilin-1 are cytoprotective. *J. Biol. Chem.* **279**, 4625-4631.
Taylor, J. P., Tanaka, F., Robitschek, J., Sandoval, C. M., Taye, A., Markovic-Plese, S. and Fischbeck, K. H. (2003). Aggresomes protect cells by enhancing the degradation of toxic polyglutamine-containing protein. *Hum. Mol. Genet.* **12**, 749-757.
Thomas, M., Yu, Z., Dadgar, N., Varambally, S., Yu, J., Chinnaiyan, A. M. and Lieberman, A. P. (2005). The unfolded protein response modulates toxicity of the expanded glutamine androgen receptor. *J. Biol. Chem.* **280**, 21264-21271.
Tomé, F. M. and Fardeau, M. (1975). Congenital myopathy with ''reducing bodies'' in muscle fibres. *Acta Neuropathol.* **31**, 207-217.
van Bebber, F., Paquet, D., Hruscha, A., Schmid, B. and Haass, C. (2010). Methylene blue fails to inhibit Tau and polyglutamine protein dependent toxicity in zebrafish. *Neurobiol. Dis.* **39**, 265-271.
Vesa, J., Su, H., Watts, G. D., Krause, S., Walter, M. C., Martin, B., Smith, C., Wallace, D. C. and Kimonis, V. E. (2009). Valosin containing protein associated inclusion body myopathy: abnormal vacuolization, autophagy and cell fusion in myoblasts. *Neuromuscul. Disord.* **19**, 766-772.
Wang, S. and Kaufman, R. J. (2012). The impact of the unfolded protein response on human disease. *J. Cell Biol.* **197**, 857-867.
Windpassinger, C., Schoser, B., Straub, V., Hochmeister, S., Noor, A., Lohberger, B., Farra, N., Petek, E., Schwarzbraun, T., Ofner, L. et al. (2008). An X-linked myopathy with postural muscle atrophy and generalized hypertrophy, termed XMPMA, is caused by mutations in FHL1. *Am. J. Hum. Genet.* **82**, 88-99.

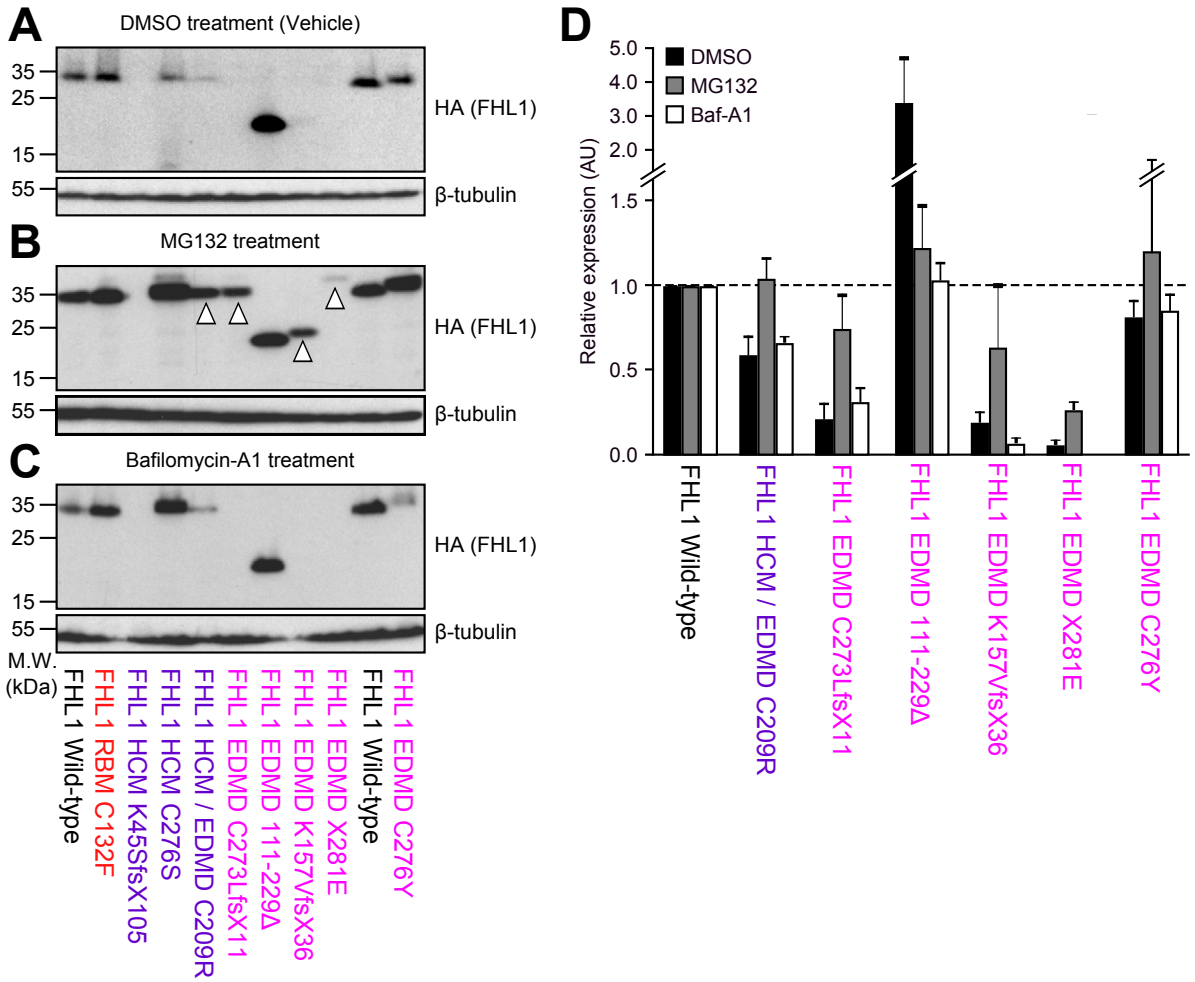

Fig. S1. HCM and EDMD HA-FHL1 mutant expression is partially restored by MG132 inhibition of the proteasome but not Bafilomycin-A1 inhibition of autophagy. C2C12 myoblasts were transiently transfected with 5 µg of DNA encoding HA-tagged wild-type, HCM or EDMD FHL1 mutants and whole cell lysates were immunoblotted with HA and β-tubulin antibodies after 48 h expression (myoblasts). Cells were treated with DMSO vehicle (A), 20 µM MG132 (B) or 5 nM Bafilomycin-A1 (C) for 24 h before harvest. Arrows show mutant HA-FHL1 expression post treatment. (D) HA-FHL1 immunoblots were analysed by densitometry and quantified relative to β-tubulin loading control and represented relative to wild-type HA-FHL1 which is represented as 1. Data represent the mean ± s.e.m. (*n*=2 for MG132 and Bafilomycin-A1 experiments, *n*=3 for DMSO control).

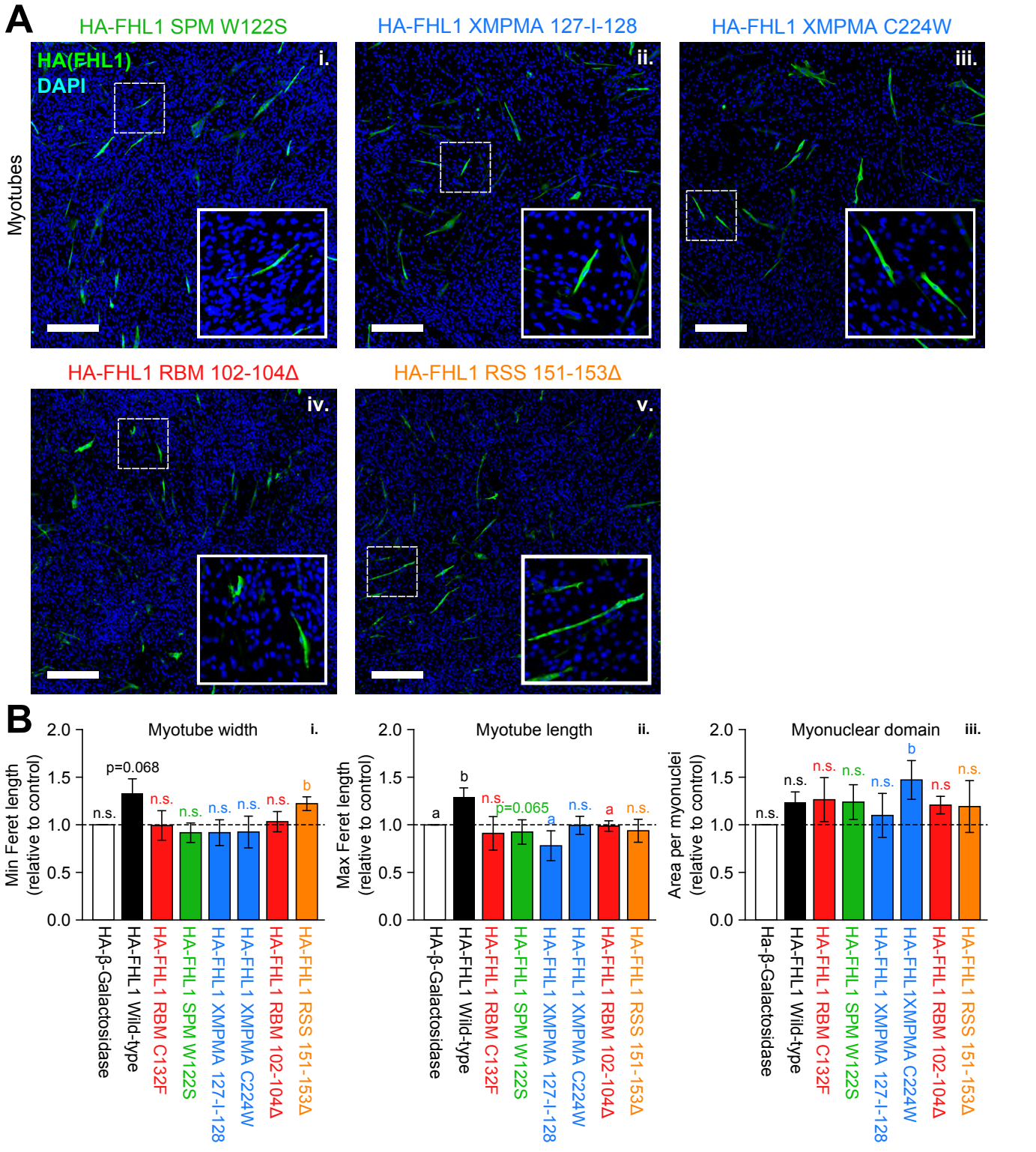

Fig. S2. RBM, SPM and XMPMA but not RSS HA-FHL1 mutants impair myoblast differentiation. Myoblast differentiation was assessed in mutant FHL1 expressing myotubes. (A) C2C12 myoblasts were transiently transfected with HA-FHL1 mutants RBM C132F (shown in Fig. 1Aiii) or RBM 102–104Δ (iv.), SPM W122S (i.), XMPMA 127-I-128 (ii.) or XMPMA C224W (iii.), RSS 151–153Δ (v.), wild-type HA-FHL1 (shown in Fig. 1Aii) or β-galactosidase control (shown in Fig. 1Ai), then differentiated for 72 h. Cells were co-stained with HA (FHL1, green), myosin heavy chain (MHC, not shown) and DAPI (nuclei, blue), then imaged by large tiled fluorescence confocal microscopy. Myotubes were defined by MHC positive staining. Scale bars: 250μm. (B) Transfected myotubes (HA-FHL1 and MHC positive cells) were assessed for myotube width (i.), length (ii.) and myonuclear domain (iii.) relative to β-galactosidase control. See Fig. 7C for myotube area, fusion index and percentage MHC+ cells. At least 100 cells per independent experiment were scored and data represent the mean percentage ± s.e.m. ($n \geq 3$; a=$P<0.05$ compared to wild-type HA-FHL1; b=$P<0.05$ compared to β-galactosidase control; n.s.=not significant).

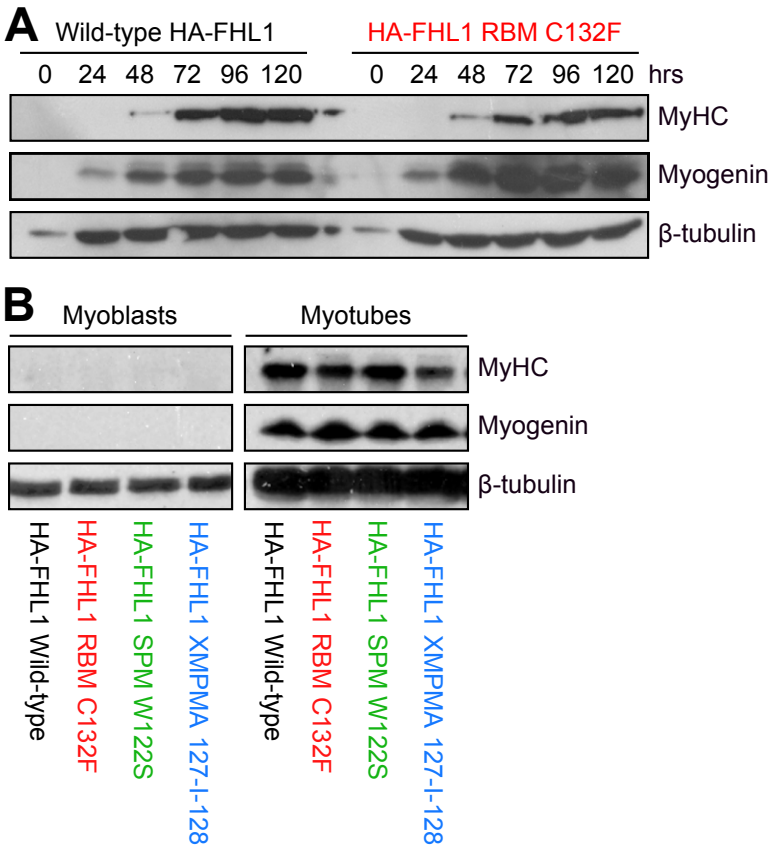

Fig. S3. RBM, SPM and XMPMA HA-FHL1 mutants do not alter expression of myosin heavy chain or myogenin. (A) Myoblast differentiation time-course was assessed in HA-FHL1 RBM C132F expressing myotubes. C2C12 myoblasts were transiently transfected with HA-FHL1 RBM C132F or wild-type HA-FHL1, then differentiated for 120 h. Whole cell lysates were immunoblotted with myosin heavy chain (MHC), myogenin or β-tubulin antibodies at 24, 48, 72, 96 and 120 h differentiation. (B) C2C12 myoblasts were transiently transfected with HA-tagged wild-type FHL1, RBM C132F, SPM W122S or XMPMA 127-I-128 (representative of each myopathy), and whole cell lysates were immunoblotted with MHC, myogenin or β-tubulin antibodies after 24 h expression (myoblasts) and after 72 h differentiation (myotubes).

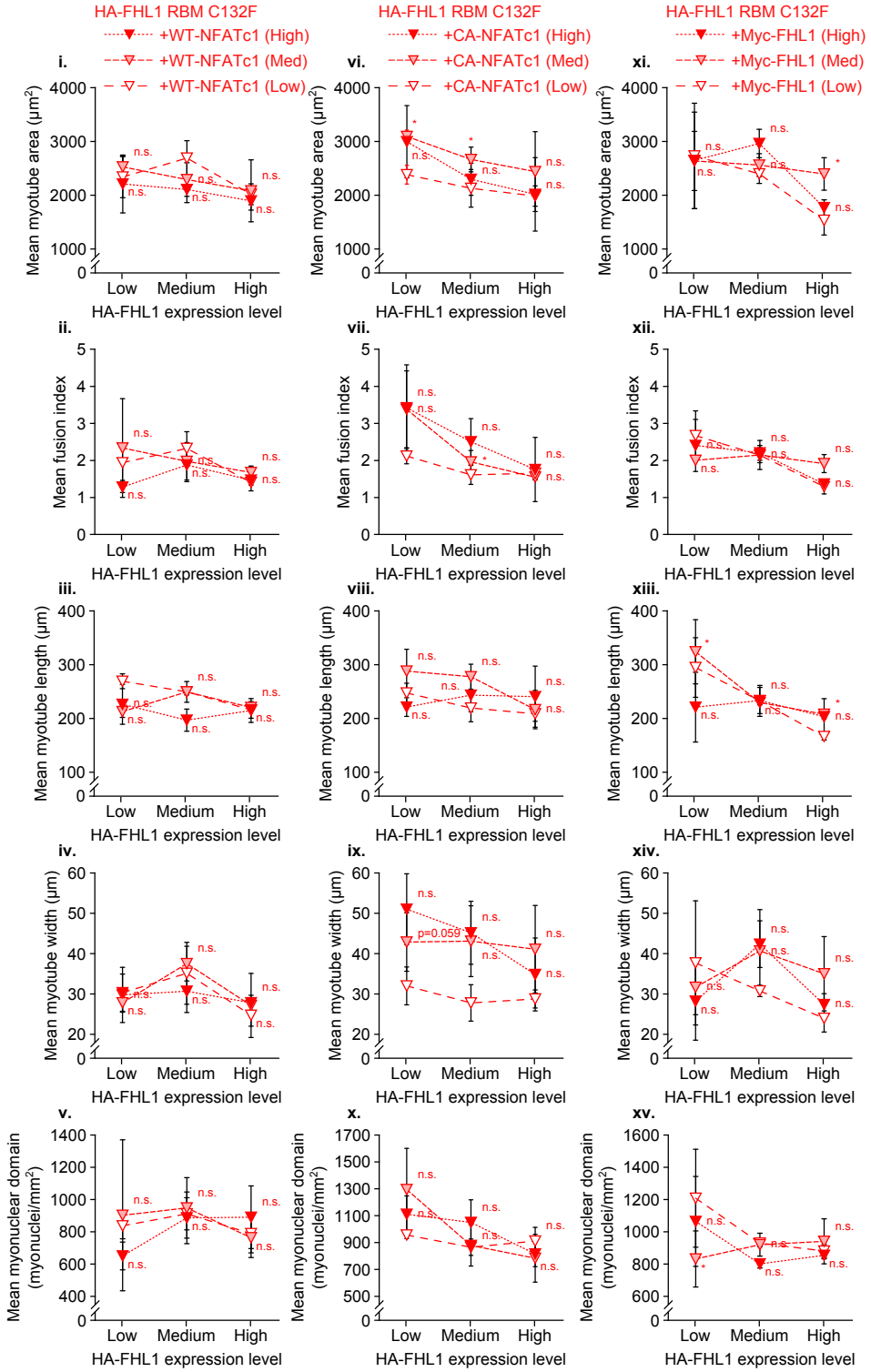

Fig. S4. Impaired differentiation of RBM mutant HA-FHL1 myotubes is rescued by expression of constitutively active NFATc1. C2C12 myoblasts were transiently co-transfected with HA-FHL1 RBM C132F, and wild-type GFP-NFATc1 (i.–v.), constitutively active GFP-NFATc1 (vi.–x.) or Myc-FHL1 (xi.–xv.), then differentiated for 72 h. Cells were co-stained with HA (568 nm), myosin heavy chain (647 nm), and DAPI (405 nm), then imaged by large tiled fluorescence confocal microscopy. Cells were manually traced in ImageJ using cytoplasmic HA-FHL1 and MHC fluorescence. NFAT/Myc expression was blindly measured by GFP fluorescence (488 nm) or Myc staining (488 nm). Each transfected myotube (HA-FHL1+/MHC+) was blindly categorised into low (<15%), medium (15–60%) or high (>60%) HA-FHL1 expression based on 568 nm average fluorescence, and blindly categorised into low (<15%), medium (15–50%) or high (>50%) rescue expression based on 488 nm average fluorescence. Myotube area, fusion index, length, width and myonuclear domain was automatically calculated in ImageJ based on individual cell tracing. At least 50 cells per independent experiment were scored and data represent the mean percentage ± s.e.m. ($n \geq 3$; paired *t*-test, *=$P<0.05$ compared to low level expression of rescue in the same HA-FHL1 RBM C132F expression level; n.s.=not significant).

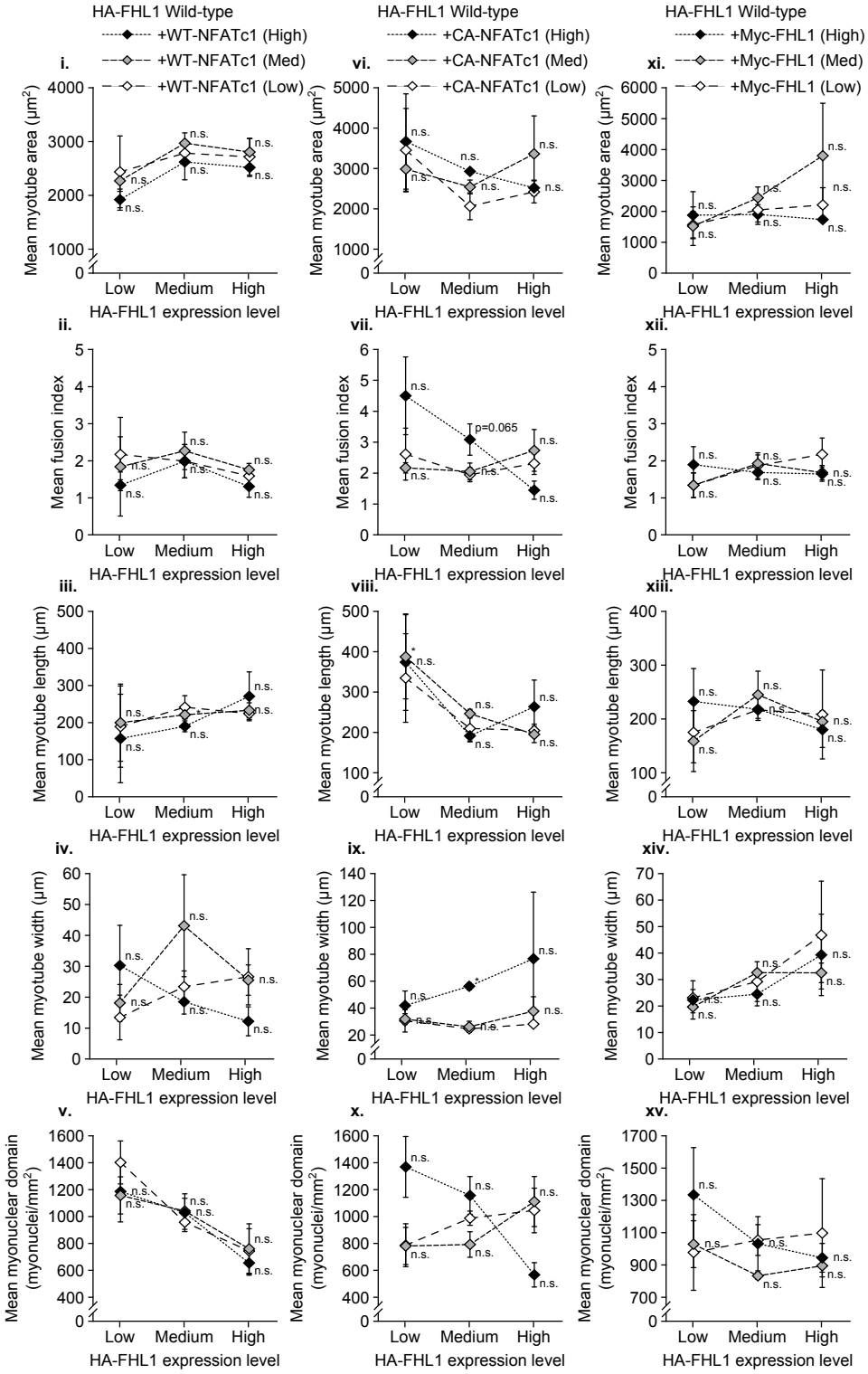

Fig. S5. Co-expression of Myc-FHL1 or GFP-NFAT does not alter differentiation in wild-type HA-FHL1 expressing myoblasts. C2C12 myoblasts were transiently co-transfected with wild-type HA-FHL1, and wild-type GFP-NFATc1 (i.–v.), constitutively active GFP-NFATc1 (vi.–x.) or Myc-FHL1 (xi.–xv.), then differentiated for 72 h. Cells were co-stained with HA (568 nm), Myosin Heavy Chain (647 nm), and DAPI (405 nm), then imaged by large tiled fluorescence confocal microscopy. Cells were manually traced in ImageJ using cytoplasmic HA-FHL1 and MHC fluorescence. NFAT/Myc expression was blindly measured by GFP fluorescence (488 nm) or Myc staining (488 nm). Each transfected myotube (HA-FHL1+/MHC+) was blindly categorised into low (<15%), medium (15–60%) or high (>60%) HA-FHL1 expression based on 568 nm average fluorescence, and blindly categorised into low (<15%), medium (15–50%) or high (>50%) rescue expression based on 488 nm average fluorescence. Myotube area, fusion index, length, width and myonuclear domain was automatically calculated in ImageJ based on individual cell tracing. At least 50 cells per independent experiment were scored and data represent the mean percentage ± s.e.m. ($n \geq 3$; paired *t*-test, *=$P<0.05$ compared to low level expression of rescue in the same wild-type HA-FHL1 expression level; n.s.=not significant).

Table S1. Summary of FHL1 myopathy mutants generated and investigated. Expression of RBM, SPM and XMPMA mutant FHL1 in affected muscle is highly variable however inheritance is generally dominant. HCM and EDMD mutant FHL1 protein expression is decreased/absent and variable penetrance is observed. Representative FHL1 mutants of each disease were investigated in this study: RBM (H123Y, C132F, C153Y, 102–104del), SPM W122S, XMPMA (127-I-128, C224W), RSS (151–153del), HCM (C209R*) and EDMD (C273LfsX11, 111–229Δ, K157VfsX36, X281E, C276Y). *The C209R missense mutation was identified in HCM with 'Emery Dreifuss-like syndrome'.

Download Table S1

Table S2. FHL1 mutation primers used to generate FHL1A myopathy mutants. Mutants representative of RBM, SPM, XMPMA, RSS, HCM and EDMD mutants were generated by PCR mutagenesis. Base-substitution, deletion and insertion mutations were introduced into wild-type FHL1 cDNA (NM_001449.3) and 5′ *Xba*I and 3′ *Xma*I restriction sites were introduced for cloning.

Download Table S2